AIMS Mathematics, 10(7): 17082–17116.
DOI: 10.3934/math.2025766
Received: 05 June 2025
Revised: 14 July 2025
Accepted: 18 July 2025
Published: 30 July 2025

https://www.aimspress.com/journal/Math

Research article

Analysis of Weibull stress-strength reliability using spacing function method under improved adaptive progressive censoring plan

Refah Alotaibi[1,*], **Ahmed Elshahhat**[2] **and Mazen Nassar**[3,4]

[1] Department of Mathematical Sciences, College of Science, Princess Nourah bint Abdulrahman University, P.O. Box 84428, Riyadh 11671, Saudi Arabia

[2] Faculty of Technology and Development, Zagazig University, Zagazig 44519, Egypt

[3] Department of Statistics, Faculty of Science, King Abdulaziz University, Jeddah 21589, Saudi Arabia

[4] Department of Statistics, Faculty of Commerce, Zagazig University, Zagazig, Egypt

* **Correspondence:** Email: rmalotaibi@pnu.edu.sa.

Abstract: Stress-strength reliability, defined as $\mathcal{R} = P(Y < X)$, plays a vital role in evaluating a system's ability to withstand stress, especially in complex engineering scenarios. This study investigated $\mathcal{R}$ when both the stress Y and strength X followed independent Weibull distributions with a common shape parameter and distinct scale parameters. The analysis was conducted under an improved adaptive progressive Type-II censoring scheme. We employed both classical and Bayesian estimation techniques. Classical inference was performed using maximum likelihood estimation and the maximum product of spacings methods, providing point and interval estimates based on their statistical properties. For Bayesian analysis, we proposed two approaches, one based on the likelihood function and the other on the spacings function, using independent gamma priors. Posterior estimates were obtained via Markov Chain Monte Carlo under a squared error loss, along with corresponding credible intervals. A comprehensive simulation study evaluated and compared the performance of the four estimators, two classical and two Bayesian, across varying censoring scenarios. The proposed methods were further validated using real-world data from organic white light-emitting diode devices, illustrating their practical utility.

Keywords: Weibull stress-strength reliability; product of spacings; improved adaptive progressive; Bayesian estimation; organic white light-emitting diode
Mathematics Subject Classification: 62F10, 62F15, 62N01, 62N02, 62N05

1. Introduction

The stress-strength reliability metric, denoted by $\mathcal{R} = P(Y < X)$, is a fundamental performance measure with widespread applications in engineering and related fields. In this context, X represents the inherent strength of a system, while Y denotes the external stress applied to it. A system is considered to fail when the applied stress exceeds its strength, that is $Y > X$. Thus, $\mathcal{R}$ quantifies the probability that the system can resist the stress during operation, serving as a key indicator of mechanical reliability. Since the seminal work of Birnbaum [1], the statistical inference of $\mathcal{R}$ has been extensively investigated and widely implemented in reliability analysis. Researchers have proposed various robust estimation methods, both parametric and nonparametric, to evaluate $\mathcal{R}$ under different assumptions and sampling schemes. The monograph by Kotz et al. [2] offered a comprehensive review of the advancements in stress-strength models.

In recent years, considerable attention has been devoted to analyzing the stress-strength reliability parameter, reflecting its growing practical importance not only in engineering applications but also in fields such as medicine and business. Sharma et al. [3] studied the stress-strength reliability index to analyze head and neck cancer data using inverse Lindley distribution. Sharma [4] investigated head and neck cancer data through generalized inverse Lindley stress–strength reliability model. Quintino et al. [5] studied asset selection based on estimating the stress–strength reliability parameter using generalized extreme value distribution. See also the work of Kotb and Al Omari [6] and Wang et al. [7], among others.

A crucial aspect of stress-strength reliability analysis is the selection of appropriate probability distributions to model the strength X and stress Y. Among the available options, the Weibull distribution stands out for its flexibility and widespread use in reliability engineering. Defined by a scale parameter θ and a shape parameter δ, the Weibull distribution is capable of capturing a wide range of hazard rate behaviors, including constant, increasing, and decreasing shapes. These hazard patterns are commonly encountered in both engineering systems and medical survival studies, making the Weibull distribution a powerful and adaptable model for real-world failure processes. For comprehensive discussions on the extensions and applications of the Weibull distribution, see Rinne [8]. Owing to its flexibility, the Weibull distribution has been extensively utilized in stress-strength reliability studies. For example, Chiodo and Mazzanti [9] studied Bayesian estimation of Weibull stress-strength model. Asgharzadeh et al. [10] considered the stress-strength reliability of Weibull distribution based on progressive Type-II censoring (PTIIC) scheme. See also, Wang and Ye [11] and Almarashi et al. [12]. If X follows the Weibull distribution, then the associated probability density function (PDF) is expressed as

$$g(x;\theta,\delta) = \theta\delta x^{\delta-1}e^{-\theta x^{\delta}}, \quad x > 0, \tag{1.1}$$

where $\theta > 0$ controls the scale, and $\delta > 0$ determines the shape of the distribution. The cumulative distribution function (CDF) corresponding to (1.1) is

$$G(x;\theta,\delta) = 1 - e^{-\theta x^{\delta}}. \tag{1.2}$$

Under the assumption that the strength X follows a Weibull distribution, say $Weibull(\theta_1, \delta)$ and the stress Y follows $Weibull(\theta_2, \delta)$, with independence between X and Y, the stress-strength reliability

parameter $\mathcal{R} = P(Y < X)$ simplifies to

$$\mathcal{R} = \frac{\theta_1}{\theta_1 + \theta_2}. \tag{1.3}$$

Investigating the stress-strength reliability index using complete data is no longer a practical approach, primarily because modern products tend to be highly reliable, often requiring extended periods before any failures are observed. Although complete data offers detailed insights, practical limitations such as time constraints and high experimental costs often make it impractical, leading to the widespread use of censored data in real-world studies. This introduces a significant challenge: identifying the most appropriate censoring scheme. The statistical literature highlights various censoring methodologies, each with distinct merits, to tackle this issue. Researchers and practitioners generally focus on approaches that achieve an optimal balance between reducing test duration and ensuring an adequate number of observed failures, enabling both accurate and efficient statistical inferences.

One of the most widely utilized censoring schemes is the progressive Type-II censoring (PT2C) plan. This methodology permits the experimenter to remove a predetermined number of surviving units at specified failure times, thereby enabling the withdrawing units to be employed for further analysis or testing. Balakrishnan and Aggarwala [13] explored a wide range of applications for progressive censoring in life testing experiments. See also the work of Balakrishnan [14]. To enhance the flexibility of this design, Kundu and Joarder [15] introduced a hybrid version that permits the experiment to conclude at the earlier of a pre-specified number of failures or a predetermined time. However, this approach may result in a minimal number of observed failures, or, in some instances, none at all, which can substantially reduce the efficiency and reliability of subsequent statistical inferences.

To address this limitation, Ng et al. [16] introduced the adaptive PT2C (APT2C) scheme, which dynamically modifies the testing protocol in response to real-time trial progress to ensure a predetermined number of failures. Although APT2C enhances the efficiency of parameter estimation when the overall duration of the trial is not of primary concern, its efficacy declines for highly reliable products. As observed by Ng et al. [16], such scenarios frequently necessitate prolonged testing periods, during which APT2C may struggle to maintain a practically manageable total test duration. See for more detail Nassar and Abo-Kasem [17], Dutta et al. [18], and Zhang et al. [19]. To overcome this limitation, Yan et al. [20] proposed the Improved APT2C (IAPT2C) scheme. Unlike earlier plans, the IAPT2C ensures that the test ends within a fixed time while still allowing flexibility during the experiment. The IAPT2C acts as a general framework that includes several existing censoring methods, making it useful in many situations. Consider an experiment involving n identical units and m (with $m < n$) represents the target number of failures to be observed, governed by a predefined censoring removal pattern $\mathbf{R} = (R_1, R_2, \ldots, R_m)$. The experimenter establishes two critical time thresholds $T^{\min}$ and $T^{\max}$, where($T^{\min} < T^{\max}$). Let the lifetimes of the test units denoted by $X_{1:m:n}, X_{2:m:n}, \ldots, X_{m:m:n}$.

The implementation of the IAPT2C is outlined as follows: Initially, at the time of each failure $X_{1:m:n}$, R_i surviving units are randomly removed, but the test adapts based on three termination scenarios:

- **Case-1:** This occurs when $X_{m:m:n} < T^{\min}$, meaning the m^{th} failure happens before the minimum allowable test duration $T^{\min}$. In this case, the test ends at $X_{m:m:n}$, resulting in a PT2C sample.
- **Case-2:** This represents the APT2C scenario, where $T^{\min} < X_{m:m:n} < T^{\max}$. Here, after observing d failures before the threshold $T^{\min}$, no further units are removed from the test until the m^{th} failure is reached. At that point, all remaining items are withdrawn from the study.

- **Case-3:** This situation arises when $T^{\min} < T^{\max} < X_{m:m:n}$, and the test concludes at the strict termination time $T^{\max}$. Similar to Case-2, no units are removed after $T^{\min}$. At $T^{\max}$, all surviving items are removed, with r failures observed before $T^{\max}$.

Recently, the IAPT2C scheme has attracted considerable attention from researchers due to its flexibility and practical relevance. For instance, Nassar and Elshahhat [21] explored estimation procedures for the Weibull distribution under this scheme. Zhang and Yan [22] investigated the Chen distribution using the IAPT2C framework. Swaroop et al. [23] examined the stress–strength reliability of the generalized inverted exponential distribution, while Irfan et al. [24] studied statistical inference for the Kumaraswamy-G family of distributions.

This research considers a comprehensive analysis of the stress-strength reliability parameter $\mathcal{R}$ for the Weibull distribution under the IAPT2C samples, integrating both classical and Bayesian methodologies. Classical estimation employs maximum likelihood (ML) and maximum product of spacings (MPS) methods to derive point and interval estimates for $\mathcal{R}$, while Bayesian inference introduces two approaches: Likelihood function-based approach (LFBA) and spacings function-based approach(SFBA), utilizing Markov Chain Monte Carlo (MCMC) sampling under squared error loss to compute posterior estimates. The study is motivated by three critical factors: (1) The broad applicability of the stress-strength reliability parameter across disciplines beyond engineering, including medicine and business. (2) The prominence of the Weibull distribution in modeling lifetime data with variable failure rates. (3) The adaptability of the IAPT2C scheme, which is particularly valuable in modern reliability testing where time constraints must be observed, offers a practical balance between flexibility and efficiency. To the best of our knowledge, this is the first study to: (i) analyze the stress-strength reliability parameter assuming both X and Y following independent Weibull distributions using IAPT2C samples, and (ii) apply the MPS and SFBA methods in this context, an approach that can be extended to other lifetime distributions as well. The ML estimates (MLE) and the MPS estimate (MPSE) of $\mathcal{R}$ are derived using the invariance property of these estimators. The approximate confidence intervals (ACIs) are also computed based on the asymptotic properties of these estimators. Bayesian estimates using the LFBA and SFBA are obtained by sampling from their respective posterior distributions, and Bayesian credible intervals (BCIs) are subsequently calculated. A comprehensive simulation study is conducted across various experimental scenarios to evaluate the accuracy of both classical and Bayesian estimation methods. Finally, real-world datasets are analyzed to demonstrate the practical applicability and significance of the proposed methodologies.

The organization of this study is as follows: In Section 2, we present the MLE of $\mathcal{R}$ along with its corresponding ACI. Section 3 investigates the MPSE and its associated ACI. Bayesian estimation techniques using the LFBA and SFBA are explored in Section 4. Section 5 evaluates the performance of these estimators through comprehensive simulation studies. In Section 6, the proposed methodologies are applied to engineering real-world datasets to demonstrate their practical utility. Finally, Section 7 outlines the key findings of the study.

2. Likelihood estimation

The MLE and ACI of the stress-strength reliability parameter $\mathcal{R}$ are discussed in this section. Let $\underline{\mathbf{x}}$ be an observed IAPT2C sample from $Weibull(\theta_1, \delta)$, with censoring plan $\mathbf{R} = (R_1, R_2, \ldots, R_{m_1})$ and thresholds $T_1^{\min}$ and $T_1^{\max}$, where $T_1^{\min} < T_1^{\max}$. Also, suppose that $\underline{\mathbf{y}}$ refers to an observed IAPT2C

sample from $Weibull(\theta_2, \delta)$, with censoring scheme $\mathbf{Q} = (Q_1, Q_2, \ldots, Q_{m_2})$ and thresholds $T_2^{\min}$ and $T_2^{\max}$, where $T_2^{\min} < T_2^{\max}$.

Based on the two observed IAPT2C samples, the likelihood function (LF) can be written as

$$L(\boldsymbol{\eta}) = \left\{\prod_{i=1}^{\mathcal{B}_1} g(x_i) \prod_{i=1}^{\mathcal{D}_1} [1 - G(x_i)]^{R_i} [1 - G(\tau_1)]^{R^\star}\right\} \left\{\prod_{i=1}^{\mathcal{B}_2} g(y_i) \prod_{i=1}^{\mathcal{D}_2} [1 - G(y_i)]^{Q_i} [1 - G(\tau_2)]^{Q^\star}\right\} \quad (2.1)$$

where $\boldsymbol{\eta} = (\theta_1, \theta_2, \delta)^\top$, $x_i = x_{i:m_1:n_1}$, $y_i = y_{i:m_2:n_2}$,

$$\mathcal{B}_j = \begin{cases} m_j, & \text{Cases I/II} \\ r_j, & \text{Case III} \end{cases}, \quad \mathcal{D}_j = \begin{cases} m_j - 1, & \text{Case I} \\ d_j, & \text{Cases II/III} \end{cases}, \ j = 1, 2,$$

$$R^\star = \begin{cases} n_1 - m_1 - \sum_{i=1}^{m_1 - 1} R_i, & \text{Case I} \\ n_1 - m_1 - \sum_{i=1}^{d_1} R_i, & \text{Case II} \\ n_1 - r_1 - \sum_{i=1}^{d_1} R_i, & \text{Case III} \end{cases}, \quad Q^\star = \begin{cases} n_2 - m_2 - \sum_{i=1}^{m_2 - 1} Q_i, & \text{Case I} \\ n_2 - m_2 - \sum_{i=1}^{d_2} Q_i, & \text{Case II} \\ n_2 - r_2 - \sum_{i=1}^{d_2} Q_i, & \text{Case III} \end{cases},$$

$$(\tau_1, \tau_2) = \begin{cases} (x_{m_1}, y_{m_2}), & \text{Cases I/II} \\ \left(T_1^{\max}, T_2^{\max}\right), & \text{Case III} \end{cases}.$$

Let $\mathcal{B} = \mathcal{B}_1 + \mathcal{B}_2$, then using (1.1), (1.2) and (2.1), we can write the LF as follows

$$L(\boldsymbol{\eta}) = \theta_1^{\mathcal{B}_1} \theta_2^{\mathcal{B}_2} \delta^{\mathcal{B}} \exp\left\{\delta \left[\sum_{i=1}^{\mathcal{B}_1} \log(x_i) + \sum_{i=1}^{\mathcal{B}_2} \log(y_i)\right] - \theta_1 \nu(\underline{\mathbf{x}}; \delta) - \theta_2 \omega(\underline{\mathbf{y}}; \delta)\right\}, \quad (2.2)$$

where

$$\nu(\underline{\mathbf{x}}; \delta) = \sum\nolimits_{i=1}^{\mathcal{B}_1} x_i^\delta + \sum\nolimits_{i=1}^{\mathcal{D}_1} R_i x_i^\delta + R^\star \tau_1^\delta$$

and

$$\omega(\underline{\mathbf{y}}; \delta) = \sum\nolimits_{i=1}^{\mathcal{B}_2} y_i^\delta + \sum\nolimits_{i=1}^{\mathcal{D}_2} Q_i y_i^\delta + Q^\star \tau_2^\delta.$$

The log-LF of (2.2) is

$$\mathcal{L}(\boldsymbol{\eta}) = \mathcal{B}_1 \log(\theta_1) + \mathcal{B}_2 \log(\theta_2) + \mathcal{B} \log(\delta) + \delta W - \theta_1 \nu(\underline{\mathbf{x}}; \delta) - \theta_2 \omega(\underline{\mathbf{y}}; \delta), \quad (2.3)$$

where $W = \sum_{i=1}^{\mathcal{B}_1} \log(x_i) + \sum_{i=1}^{\mathcal{B}_2} \log(y_i)$. The MLEs of θ_1, θ_2 and δ, denoted by $\hat{\theta}_1, \hat{\theta}_2$ and $\hat{\delta}$, can be derived as the solution of the following three likelihood equations

$$\frac{\mathcal{B}_1}{\theta_1} - \nu(\underline{\mathbf{x}}; \delta) = 0, \quad \frac{\mathcal{B}_2}{\theta_2} - \omega(\underline{\mathbf{y}}; \delta) = 0 \quad (2.4)$$

and

$$\frac{\mathcal{B}}{\delta} + W - \theta_1 \nu_1(\underline{\mathbf{x}}; \delta) - \theta_2 \omega_1(\underline{\mathbf{y}}; \delta) = 0, \quad (2.5)$$

where

$$\nu_1(\underline{\mathbf{x}}; \delta) = \sum\nolimits_{i=1}^{\mathcal{B}_1} x_i^\delta \log(x_i) + \sum\nolimits_{i=1}^{\mathcal{D}_1} R_i x_i^\delta \log(x_i) + R^\star \tau_1^\delta \log(\tau_1)$$

and

$$\omega_1(\underline{\mathbf{y}};\delta) = \sum_{i=1}^{\mathcal{B}_2} y_i^{\delta}\log(y_i) + \sum_{i=1}^{\mathcal{D}_2} Q_i y_i^{\delta}\log(y_i) + Q^{\star}\tau_2^{\delta}\log(\tau_2).$$

From the two normal equations in (2.4), the MLEs of $\hat{\theta}_1$ and $\hat{\theta}_2$ can be derived explicitly as a function of the unknown shape parameter δ as

$$\hat{\theta}_1(\delta) = \frac{\mathcal{B}_1}{\nu(\underline{\mathbf{x}};\delta)}, \text{ and } \hat{\theta}_2(\delta) = \frac{\mathcal{B}_2}{\omega(\underline{\mathbf{y}};\delta)}. \tag{2.6}$$

The MLE of the shape parameter, denoted by $\hat{\delta}$, can be computed as the solution of $\xi(\delta) = \delta$, which derived after replacing the MLEs $\hat{\theta}_1(\delta)$ and $\hat{\theta}_2(\delta)$ given by (2.6) into the normal equation in (2.5), as

$$\xi(\delta) = \left[\frac{\mathcal{B}_1\frac{\nu_1(\underline{\mathbf{x}};\delta)}{\nu(\underline{\mathbf{x}};\delta)} + \mathcal{B}_2\frac{\omega_1(\underline{\mathbf{y}};\delta)}{\omega(\underline{\mathbf{y}};\delta)} - W}{\mathcal{B}}\right]^{-1}. \tag{2.7}$$

The MLE $\hat{\delta}$ can be easily acquired by utilizing the iterative method, provided as $\xi(\delta^{(j)}) = \delta^{(j+1)}$, where $\delta^{(j)}$ refers to the j-th iteration, to solve (2.7). Upon getting the MLE $\hat{\delta}$, the MLEs of θ_1 and θ_2 can be computed using (2.6) as $\hat{\theta}_1 = \hat{\theta}_1(\hat{\delta})$ and $\hat{\theta}_2 = \hat{\theta}_2(\hat{\delta})$. Immediately, after calculating the MLEs of the model parameters $\hat{\theta}_1, \hat{\theta}_2$ and $\hat{\delta}$, the invariance property can be used in order to compute the MLE of the stress-strength reliability parameter $\mathcal{R}$ using (1.3), after some simplifications, as follows:

$$\hat{\mathcal{R}} = \left[1 + \frac{\mathcal{B}_2\nu(\underline{\mathbf{x}};\hat{\delta})}{\mathcal{B}_1\omega(\underline{\mathbf{y}};\hat{\delta})}\right]^{-1}.$$

Another critical aspect in analyzing the stress-strength reliability parameter $\mathcal{R}$, involves constructing confidence intervals that capture the true parameter value with a specified probability. To achieve this, we employ the asymptotic normality of MLEs and apply the delta method to approximate the variance of the MLE of $\mathcal{R}$. This approach necessitates deriving the variance-covariance matrix of the MLEs for the underlying model parameters. Due to the complexity of exact analytical expressions for the Fisher information matrix, we instead compute its observed version, evaluated at the MLEs, and invert it to obtain the estimated variance-covariance matrix. This matrix is then used to approximate the standard error of $\hat{\mathcal{R}}$, enabling the construction of the ACI for $\mathcal{R}$. Thus, the estimated variance-covariance matrix, evaluated at $\hat{\boldsymbol{\eta}} = (\hat{\theta}_1, \hat{\theta}_2, \hat{\delta})^{\top}$, can be obtained as

$$\boldsymbol{\Sigma}(\hat{\boldsymbol{\eta}}) = \begin{bmatrix} -\mathcal{L}_{11} & 0 & -\mathcal{L}_{13} \\ & -\mathcal{L}_{22} & -\mathcal{L}_{23} \\ & & -\mathcal{L}_{33} \end{bmatrix}^{-1} = \begin{bmatrix} \hat{\sigma}_{11} & 0 & \hat{\sigma}_{13} \\ & \hat{\sigma}_{22} & \hat{\sigma}_{23} \\ & & \hat{\sigma}_{33} \end{bmatrix}, \tag{2.8}$$

where

$$\mathcal{L}_{11} = -\frac{\mathcal{B}_1}{\theta_1^2}, \quad \mathcal{L}_{22} = -\frac{\mathcal{B}_2}{\theta_2^2}$$

$$\mathcal{L}_{33} = -\frac{\mathcal{B}}{\delta^2} - \theta_1\nu_2(\underline{\mathbf{x}};\delta) - \theta_2\omega_2(\underline{\mathbf{y}};\delta),$$

$$\mathcal{L}_{13} = -\nu_1(\underline{\mathbf{x}}; \delta) \quad \text{and} \quad \mathcal{L}_{23} = -\omega_1(\underline{\mathbf{y}}; \delta),$$

where

$$\nu_2(\underline{\mathbf{x}}; \delta) = \sum_{i=1}^{\mathcal{B}_1} x_i^{\delta} \log^2(x_i) + \sum_{i=1}^{\mathcal{D}_1} R_i x_i^{\delta} \log^2(x_i) + R^{\star} \tau_1^{\delta} \log^2(\tau_1)$$

and

$$\omega_2(\underline{\mathbf{y}}; \delta) = \sum_{i=1}^{\mathcal{B}_2} y_i^{\delta} \log^2(y_i) + \sum_{i=1}^{\mathcal{D}_2} Q_i y_i^{\delta} \log^2(y_i) + Q^{\star} \tau_2^{\delta} \log^2(\tau_2).$$

The delta method approximates the variance of the MLE of $\mathcal{R}$ by employing the asymptotic properties of the MLEs and the functional relationship of $\mathcal{R}$ to the model parameters. Specifically, if $\mathcal{R} = f(\boldsymbol{\eta})$, then the variance of $\hat{\mathcal{R}}$ is approximated as

$$\widehat{Var}(\hat{\mathcal{R}}) \approx [\nabla f(\hat{\boldsymbol{\eta}})]^{\top} \boldsymbol{\Sigma}(\hat{\boldsymbol{\eta}}) [\nabla f(\boldsymbol{\eta})],$$

where $\nabla f(\hat{\boldsymbol{\eta}})$ is the gradient vector of $f(\boldsymbol{\eta})$ evaluated at the MLE $\hat{\boldsymbol{\eta}}$. Accordingly, $\widehat{Var}(\hat{\mathcal{R}})$ can be simplified as

$$\begin{aligned} \widehat{Var}(\hat{\mathcal{R}}) &\simeq \frac{1}{(\hat{\theta}_1 + \hat{\theta}_2)^2} \left[\hat{\theta}_2, -\hat{\theta}_1, 0\right] \begin{bmatrix} \hat{\sigma}_{11} & 0 & \hat{\sigma}_{13} \\ & \hat{\sigma}_{22} & \hat{\sigma}_{23} \\ & & \hat{\sigma}_{33} \end{bmatrix} \begin{bmatrix} \hat{\theta}_2 \\ -\hat{\theta}_1 \\ 0 \end{bmatrix} \\ &\simeq \frac{\hat{\theta}_1^2 \hat{\sigma}_{22} + \hat{\theta}_2^2 \hat{\sigma}_{11}}{(\hat{\theta}_1 + \hat{\theta}_2)^2}. \end{aligned}$$

Let α refer to the significance level, then the $100\%(1-\alpha)$ ACI of $\mathcal{R}$ can be calculated as

$$\left(\frac{\hat{\theta}_1 - z_{\alpha/2} \sqrt{\hat{\theta}_1^2 \hat{\sigma}_{22} + \hat{\theta}_2^2 \hat{\sigma}_{11}}}{\hat{\theta}_1 + \hat{\theta}_2}, \frac{\hat{\theta}_1 + z_{\alpha/2} \sqrt{\hat{\theta}_1^2 \hat{\sigma}_{22} + \hat{\theta}_2^2 \hat{\sigma}_{11}}}{\hat{\theta}_1 + \hat{\theta}_2} \right),$$

where $z_{\alpha/2}$ is the upper $(\alpha/2)^{th}$ quantile point of $N(0, 1)$.

3. Product of spacings estimation

The MPS method, introduced independently by Cheng and Amin [25] and Ranneby [26], offers a robust alternative to traditional ML estimation, especially in scenarios where the ML method may break down, such as in the case of complex distributions. In such cases, ML method can yield inconsistent estimators, while MPS method remains stable. The MPS method is based on the concept of spacings, which are defined as the differences between the CDF values of consecutive ordered data points. In this approach, MPSEs are obtained by maximizing the spacing function (SF) in the sample, following a principle analogous to the likelihood maximization used in ML estimation. As shown by Anatolyev and Kosenok [27], MPSEs often demonstrate greater efficiency than MLEs, especially in the presence of skewed distributions or small sample sizes, where likelihood-based estimators may perform poorly. Cheng and Amin [25] showed that MPSEs and MLEs are asymptotically equivalent and share key desirable properties such as asymptotic sufficiency, consistency, and efficiency. Ranneby [26] showed

that the MPSEs possess invariance and consistency properties similar to MLEs and often perform comparably in large samples. See for more detail, Kurdi et al. [28].

Based on the two IAPT2C samples obtained from the Weibull populations, with the same notation described in the previous section, we can write the SF as follows:

$$P(\boldsymbol{\eta}) = \left\{\prod_{i=1}^{\mathcal{B}_1+1}\Delta(x_i)\prod_{i=1}^{\mathcal{D}_1}[1-G(x_i)]^{R_i}[1-G(\tau_1)]^{R^\star}\right\}\left\{\prod_{i=1}^{\mathcal{B}_2+1}\Delta(y_i)\prod_{i=1}^{\mathcal{D}_2}[1-G(y_i)]^{Q_i}[1-G(\tau_2)]^{Q^\star}\right\}, \tag{3.1}$$

where $\Delta(x_i) = F(x_i) - F(x_{i-1})$ and $\Delta(y_i) = F(y_i) - F(y_{i-1})$. Based on (1.1), (1.2) and (3.1), SF can be written as follows

$$P(\boldsymbol{\eta}) = \exp\left\{\sum_{i=1}^{\mathcal{B}_1+1}\log\left(e^{\theta_1 a_i}-1\right)+\sum_{i=1}^{\mathcal{B}_2+1}\log\left(e^{\theta_2 b_i}-1\right)-\theta_1\nu(\underline{\mathbf{x}};\delta)-\theta_2\omega(\underline{\mathbf{y}};\delta)\right\}, \tag{3.2}$$

where $a_i = x_i^\delta - x_{i-1}^\delta$ and $b_i = y_i^\delta - y_{i-1}^\delta$. The log-SF of (3.2) can be written as

$$\mathcal{P}(\boldsymbol{\eta}) = \sum_{i=1}^{\mathcal{B}_1+1}\log\left(e^{\theta_1 a_i}-1\right)+\sum_{i=1}^{\mathcal{B}_2+1}\log\left(e^{\theta_2 b_i}-1\right)-\theta_1\nu(\underline{\mathbf{x}};\delta)-\theta_2\omega(\underline{\mathbf{y}};\delta). \tag{3.3}$$

The MPSEs of θ_1, θ_2, and δ, denoted as $\tilde{\theta}_1$, $\tilde{\theta}_2$, and $\tilde{\delta}$, can be obtained by solving the following system of three normal equations

$$\sum\nolimits_{i=1}^{\mathcal{B}_1+1}\frac{a_i}{1-e^{-\theta_1 a_i}}-\nu(\underline{\mathbf{x}};\delta)=0, \tag{3.4}$$

$$\sum\nolimits_{i=1}^{\mathcal{B}_2+1}\frac{b_i}{1-e^{-\theta_2 b_i}}-\omega(\underline{\mathbf{y}};\delta)=0 \tag{3.5}$$

and

$$\sum\nolimits_{i=1}^{\mathcal{B}_1+1}\frac{\theta_1 a_i^*}{1-e^{-\theta_1 a_i}}+\sum\nolimits_{i=1}^{\mathcal{B}_2+1}\frac{\theta_2 b_i^*}{1-e^{-\theta_2 b_i}}-\theta_1\nu_1(\underline{\mathbf{x}};\delta)-\theta_2\omega_1(\underline{\mathbf{y}};\delta)=0, \tag{3.6}$$

where $a_i^* = x_i^\delta\log(x_i) - x_{i-1}^\delta\log(x_{i-1})$ and $b_i^* = y_i^\delta\log(y_i) - y_{i-1}^\delta\log(y_{i-1})$.

It is clear from (3.4) and (3.5) that the MPSEs of θ_1, θ_2 and δ, denoted by $\tilde{\theta}_1, \tilde{\theta}_2$ and $\tilde{\delta}$, cannot be obtained explicitly due to the complexity of the normal equations. Therefore, we employ the Newton-Raphson method to compute them numerically. Once the required MPSEs are obtained, the MPSE of the stress-strength reliability parameter $\mathcal{R}$ can be calculated using the invariance property, as follows:

$$\tilde{\mathcal{R}} = \frac{\tilde{\theta}_1}{\tilde{\theta}_1+\tilde{\theta}_2}.$$

As with the ML estimation case, constructing the ACI for the stress-strength reliability parameter $\mathcal{R}$ requires the variance of the MPSE $\tilde{\mathcal{R}}$. To approximate this variance, we apply the delta method as outlined in the previous section. To accomplish this, we first obtain the estimated variance-covariance matrix evaluated at the MPSEs as

$$\boldsymbol{\Sigma}^*(\tilde{\boldsymbol{\eta}}) = \begin{bmatrix} -\mathcal{P}_{11} & 0 & -\mathcal{P}_{13} \\ & -\mathcal{P}_{22} & -\mathcal{P}_{23} \\ & & -\mathcal{P}_{33} \end{bmatrix}^{-1} = \begin{bmatrix} \hat{\sigma}_{11}^* & 0 & \hat{\sigma}_{13}^* \\ & \hat{\sigma}_{22}^* & \hat{\sigma}_{23}^* \\ & & \hat{\sigma}_{33}^* \end{bmatrix}, \tag{3.7}$$

where

$$\mathcal{P}_{11} = \sum_{i=1}^{\mathcal{B}_1+1} \frac{a_i^2 e^{-\theta_1 a_i}}{(1-e^{-\theta_1 a_i})^2}, \quad \mathcal{P}_{22} = \sum_{i=1}^{\mathcal{B}_2+1} \frac{b_i^2 e^{-\theta_2 b_i}}{(1-e^{-\theta_2 b_i})^2},$$

$$\mathcal{P}_{33} = \sum_{i=1}^{\mathcal{B}_1+1} \varrho_i + \sum_{i=1}^{\mathcal{B}_2+1} \varpi_i - \theta_1 \nu_2(\underline{\mathbf{x}}; \delta) - \theta_2 \omega_2(\underline{\mathbf{y}}; \delta) = 0,$$

$$\mathcal{P}_{13} = \sum_{i=1}^{\mathcal{B}_1+1} \frac{a_i^*}{1-e^{-\theta_1 a_i}} \left(1 - \frac{\theta_1 a_i e^{-\theta_1 a_i}}{1-e^{-\theta_1 a_i}}\right) - \nu_1(\underline{\mathbf{x}}; \delta)$$

and

$$\mathcal{P}_{23} = \sum_{i=1}^{\mathcal{B}_2+1} \frac{b_i^*}{1-e^{-\theta_2 b_i}} \left(1 - \frac{\theta_2 b_i e^{-\theta_2 b_i}}{1-e^{-\theta_2 b_i}}\right) - \omega_1(\underline{\mathbf{y}}; \delta),$$

where

$$\varrho_i = \frac{\theta_1 a_i^{**}}{1-e^{-\theta_1 a_i}} - \frac{(\theta_1 a_i^*)^2 e^{-\theta_1 a_i}}{(1-e^{-\theta_1 a_i})^2}, \quad \varpi_i = \frac{\theta_2 b_i^{**}}{1-e^{-\theta_2 b_i}} - \frac{(\theta_2 b_i^*)^2 e^{-\theta_2 b_i}}{(1-e^{-\theta_2 b_i})^2}$$

$a_i^{**} = x_i^{\delta} \log^2(x_i) - x_{i-1}^{\delta} \log^2(x_{i-1})$, and $b_i^{**} = y_i^{\delta} \log^2(y_i) - y_{i-1}^{\delta} \log^2(y_{i-1})$.

Then, after applying the delta method we can approximate the required variance of the MPSE of $\tilde{\mathcal{R}}$ as

$$\widetilde{Var}(\tilde{\mathcal{R}}) \simeq \frac{\tilde{\theta}_1^2 \tilde{\sigma}_{22}^* + \tilde{\theta}_2^2 \tilde{\sigma}_{11}^*}{(\tilde{\theta}_1 + \tilde{\theta}_2)^2}.$$

Accordingly, the $100\%(1-\alpha)$ ACI of $\mathcal{R}$ is

$$\left(\frac{\tilde{\theta}_1 - z_{\alpha/2} \sqrt{\tilde{\theta}_1^2 \tilde{\sigma}_{22}^* + \tilde{\theta}_2^2 \tilde{\sigma}_{11}^*}}{\tilde{\theta}_1 + \tilde{\theta}_2}, \frac{\tilde{\theta}_1 + z_{\alpha/2} \sqrt{\tilde{\theta}_1^2 \tilde{\sigma}_{22}^* + \tilde{\theta}_2^2 \tilde{\sigma}_{11}^*}}{\tilde{\theta}_1 + \tilde{\theta}_2} \right).$$

4. Bayesian estimation

In this section, two Bayesian estimation approaches are considered as alternatives to the ML and MPS methods. These approaches are based on the LFBA and the SFBA, which offer two different frameworks for deriving the posterior distributions of the unknown parameters. We assume that the three parameters are independent and each follows a gamma prior distribution. Notably, under the likelihood function, the gamma distribution serves as a conjugate prior for each scale parameter. However, no natural conjugate prior exists for the shape parameter. Therefore, we take advantage of the flexibility of the gamma distribution and adopt it as a prior for the shape parameter as well.

Let $\theta_1 \sim Gamma(\lambda_1, \beta_1)$, $\theta_2 \sim Gamma(\lambda_2, \beta_2)$ and $\delta \sim Gamma(\lambda_3, \beta_3)$. Therefore, the joint prior distribution of $\boldsymbol{\eta}$ follows

$$\pi(\boldsymbol{\eta}) \propto \theta_1^{\lambda_1-1}\theta_2^{\lambda_2-1}\delta^{\lambda_3-1}\exp\{\beta_1\theta_1 - \beta_2\theta_2 - \beta_3\delta\},\ \theta_1, \theta_2, \delta > 0, \tag{4.1}$$

where $\lambda_j, \beta_j > 0, j = 1, 2$, are the hyper-parameters. Employing the LF in (2.2), the posterior distribution using the LFBA can be derived after combining the LF with the prior distribution in (4.1) as follows

$$H_1(\boldsymbol{\eta}|\underline{\mathbf{x}}, \underline{\mathbf{y}}) = \frac{\theta_1^{\mathcal{B}_1+\lambda_1-1}\theta_2^{\mathcal{B}_2+\lambda_2-1}\delta^{\mathcal{B}+\lambda_3-1}}{A_1}\exp\left\{\delta(W-\beta_3) - \theta_1[\nu(\underline{\mathbf{x}};\delta)+\beta_1] - \theta_2[\omega(\underline{\mathbf{y}};\delta)+\beta_2]\right\}, \tag{4.2}$$

where A_1 is the normalized constant. On the other hand, the posterior distribution using the SFBA can be acquired using (3.2) and (4.1) as

$$\begin{aligned} H_2(\boldsymbol{\eta}|\underline{\mathbf{x}}, \underline{\mathbf{y}}) = {} & \frac{1}{A_2}\theta_1^{\lambda_1-1}\theta_2^{\lambda_2-1}\delta^{\lambda_3-1}\exp\left\{\sum_{i=1}^{\mathcal{B}_1+1}\log\left(e^{\theta_1 a_i}-1\right) + \sum_{i=1}^{\mathcal{B}_2+1}\log\left(e^{\theta_2 b_i}-1\right)\right. \\ & \left. - \theta_1[\nu(\underline{\mathbf{x}};\delta)+\beta_1] - \theta_2[\omega(\underline{\mathbf{y}};\delta)+\beta_2] - \beta_3\delta\right\}, \end{aligned} \tag{4.3}$$

where A_2 refers to the normalized constant.

Based on the squared error loss function, the Bayes estimator of $\mathcal{R}$ is given by the posterior mean. However, obtaining this estimator analytically is challenging due to the lack of closed-form expressions for the two posterior distributions. To overcome this difficulty, numerical techniques such as the MCMC methods are employed. These methods generate samples from the posterior distribution, allowing for a numerical approximation of $\mathcal{R}$. We begin with the posterior distribution derived using LFBA. A crucial step involves constructing the full conditional distributions from the joint posterior density in (4.2), which are then used to iteratively sample the model parameters. The Bayes estimate of $\mathcal{R}$ and the corresponding BCI are then approximated using summaries of the posterior distribution. Using the posterior distribution in (4.2), we observe that

$$\theta_1 \sim Gamma\left(\mathcal{B}_1 + \lambda_1, \nu(\underline{\mathbf{x}};\delta) + \beta_1\right) \tag{4.4}$$

$$\theta_2 \sim Gamma\left(\mathcal{B}_2 + \lambda_2, \omega(\underline{\mathbf{y}};\delta) + \beta_2\right) \tag{4.5}$$

and

$$H_1(\delta|\boldsymbol{\eta}_{-\delta}, \underline{\mathbf{x}}, \underline{\mathbf{y}}) \propto \delta^{\mathcal{B}+\lambda_3-1}\exp\left\{\delta(W-\beta_3) - \theta_1\nu(\underline{\mathbf{x}};\delta) - \theta_2\omega(\underline{\mathbf{y}};\delta)\right\}. \tag{4.6}$$

From (4.4) and (4.5), it is clear that sampling for θ_1 and θ_2 can be carried out directly using any sampling generation routine. On the other hand, as given in (4.6), the full conditional distribution of δ does not align with any standard statistical distribution. To address this, we utilize the Metropolis-Hastings (M-H) algorithm using a normal proposal distribution within the Gibbs sampler to generate the necessary MCMC samples. The following steps outline the implementation of the proposed hybrid algorithm:

Algorithm 1

Step 1. Set $k = 1$ and $\left(\theta_1^{(0)}, \theta_2^{(0)}, \delta^{(0)}\right) = \left(\hat{\theta}_1, \hat{\theta}_2, \hat{\delta}\right)$.
Step 2. Get $\delta^{(k)}$ employing $H_1(\delta|\boldsymbol{\eta}_{-\delta}, \underline{\mathbf{x}}, \underline{\mathbf{y}})$ in (4.6) using the M-H steps:
- Obtain δ^* using $N\left(\delta^{(k-1)}, \hat{\sigma}_{33}\right)$.
- Calculate the acceptance ratio:

$$\phi_1 = \min\left[1, \frac{H_1(\delta^*|\theta_1^{(k-1)}, \theta_2^{(k-1)}, \underline{\mathbf{x}}, \underline{\mathbf{y}})}{H_1(\delta^{(k-1)}|\theta_1^{(k-1)}, \theta_2^{(k-1)}, \underline{\mathbf{x}}, \underline{\mathbf{y}})}\right].$$

- Simulate u using $U(0, 1)$.
- If $u \leq \phi_1$, put $\delta^{(k)} = \delta^*$. Otherwise, put $\delta^{(k)} = \delta^{(k-1)}$.

Step 3. Obtain $\theta_1^{(k)}$ using $Gamma\left(\mathcal{B}_1 + \lambda_1, \nu(\underline{\mathbf{x}}; \delta^{(k)}) + \beta_1\right)$.
Step 4. Generate $\theta_2^{(k)}$ from $Gamma\left(\mathcal{B}_2 + \lambda_2, \omega(\underline{\mathbf{y}}; \delta^{(k)}) + \beta_2\right)$.
Step 5. Obtain the value of $\mathcal{R}$ at iteration k as follows:

$$\mathcal{R}^{(k)} = \frac{\theta_1^{(k)}}{\theta_1^{(k)} + \theta_2^{(k)}}.$$

Step 6. Update j by $j + 1$.
Step 7. Redo Steps 2 to 6, $\mathcal{M}$ times to obtain $\left\{\mathcal{R}^{(1)}, \mathcal{R}^{(2)}, \ldots, \mathcal{R}^{(\mathcal{M})}\right\}$.

Then we can compute the Bayes estimate of $\mathcal{R}$ using the LFBA, denoted by $\hat{\mathcal{R}}_B$ as

$$\hat{\mathcal{R}}_B = \frac{1}{\mathcal{M} - C} \sum_{k=C+1}^{\mathcal{M}} \mathcal{R}^{(k)},$$

where C is the burn-in period. To compute the $100\%(1-\alpha)$ BCI of $\mathcal{R}$, sort the obtained MCMC samples in ascending order as $\left\{\mathcal{R}^{[C+1]} < \mathcal{R}^{[2]} < \cdots < \mathcal{R}^{[\mathcal{M}]}\right\}$. Then, calculate the $100\%(1-\alpha)$ BCI as

$$\left\{\mathcal{R}^{[\alpha(\mathcal{M}-C)/2]}, \mathcal{R}^{[(1-\alpha/2)(\mathcal{M}-C)]}\right\}.$$

Similar to the procedure used to obtain the Bayes point estimate and BCI of the stress-strength reliability parameter $\mathcal{R}$ under the LFBA, the corresponding estimates can also be derived using the SFBA. The first step in this approach is to formulate the full conditional distributions of the unknown parameters based on the posterior distribution given in (4.3), as follows

$$H_2(\theta_1|\boldsymbol{\eta}_{-\theta_1}, \underline{\mathbf{x}}, \underline{\mathbf{y}}) \propto \theta_1^{\lambda_1 - 1} \exp\left\{\sum\nolimits_{i=1}^{\mathcal{B}_1+1} \log\left(e^{\theta_1 a_i} - 1\right) - \theta_1[\nu(\underline{\mathbf{x}}; \delta) + \beta_1]\right\}, \tag{4.7}$$

$$H_2(\theta_2|\boldsymbol{\eta}_{-\theta_1}, \underline{\mathbf{x}}, \underline{\mathbf{y}}) \propto \theta_2^{\lambda_2 - 1} \exp\left\{\sum\nolimits_{i=1}^{\mathcal{B}_2+1} \log\left(e^{\theta_2 b_i} - 1\right) - \theta_2[\omega(\underline{\mathbf{y}}; \delta) + \beta_2]\right\} \tag{4.8}$$

and

$$\begin{aligned} H_2(\delta|\boldsymbol{\eta}_{-\delta}, \underline{\mathbf{x}}, \underline{\mathbf{y}}) \propto\ & \delta^{\lambda_3 - 1} \exp\left\{\sum\nolimits_{i=1}^{\mathcal{B}_1+1} \log\left(e^{\theta_1 a_i} - 1\right) + \sum\nolimits_{i=1}^{\mathcal{B}_2+1} \log\left(e^{\theta_2 b_i} - 1\right)\right. \\ & \left. - \theta_1 \nu(\underline{\mathbf{x}}; \delta) - \theta_2 \omega(\underline{\mathbf{y}}; \delta) - \beta_3 \delta\right\} \end{aligned} \tag{4.9}$$

As seen from (4.7)–(4.9), none of the three full conditional distributions correspond to any known statistical distribution. Therefore, we use the M-H steps, as provided in Step 2 of Algorithm 1, to simulate the MCMC samples in this case. For each parameter, a normal proposal distribution is utilized. The steps below describe the process for generating the samples (see Algorithm 2):

Algorithm 2

Step 1. Put $k = 1$ and $\left(\theta_1^{(0)}, \theta_2^{(0)}, \delta^{(0)}\right) = \left(\tilde{\theta}_1, \tilde{\theta}_2, \tilde{\delta}\right)$.
Step 2. Simulate $\theta_1^{(k)}$ through the M-H steps using $H_2(\theta_1|\boldsymbol{\eta}_{-\theta_1}, \underline{\mathbf{x}}, \underline{\mathbf{y}})$ in (4.7) .
Step 3. Generate $\theta_2^{(k)}$ via the M-H algorithm employing $H_2(\theta_2|\boldsymbol{\eta}_{-\theta_1}, \underline{\mathbf{x}}, \underline{\mathbf{y}})$ in (4.8) .
Step 4. Compute $\delta^{(k)}$ using the M-H steps utilizing $H_2(\delta|\boldsymbol{\eta}_{-\delta}, \underline{\mathbf{x}}, \underline{\mathbf{y}})$ in (4.9) .
Step 5. Compute $\mathcal{R}^{*(k)}$ as:

$$\mathcal{R}^{*(k)} = \frac{\theta_1^{(k)}}{\theta_1^{(k)}+\theta_2^{(k)}}.$$

Step 6. Put $k = k + 1$.
Step 7. Repeat Steps 2 to 6 $\mathcal{M}$ times to compute $\left\{\mathcal{R}^{*(1)}, \mathcal{R}^{*(2)}, \ldots, \mathcal{R}^{*(\mathcal{M})}\right\}$.

Then, the Bayes estimate of $\mathcal{R}$ based on the SFBA, denoted by $\tilde{\mathcal{R}}_B$, can be obtained as

$$\tilde{\mathcal{R}}_B = \frac{1}{\mathcal{M}-C}\sum\nolimits_{k=C+1}^{\mathcal{M}} \mathcal{R}^{*(k)},$$

In addition, by sorting the MCMC samples as $\left\{\mathcal{R}^{*[\mathcal{B}+1]} < \mathcal{R}^{*[2]} < \cdots < \mathcal{R}^{*[\mathcal{M}]}\right\}$, the $100\%(1-\alpha)$ BCI of $\mathcal{R}$ can be computed as

$$\left\{\mathcal{R}^{*[\alpha(\mathcal{M}-C)/2]}, \mathcal{R}^{*[(1-\alpha/2)(\mathcal{M}-C)]}\right\}.$$

5. Monte Carlo simulations

This section offers comprehensive Monte Carlo simulations to assess the validity of the provided estimates for the new theoretical findings presented in the beforehand parts. To evaluate the performance of the point and interval estimators for the parameters $\theta_i,\ i = 1, 2, \delta$, and the stress-strength reliability measure $\mathcal{R}$, a simulation study was conducted using 1,000 independent IAPT2C samples. These samples were drawn from two distinct populations governed by the Weibull$(\theta_1, \theta_2, \delta)$ model, specifically defined as Group–A: $(0.4, 0.8, 0.5)$ and Group–B: $(1, 2, 1.5)$. For analytical purposes, the corresponding reference value of the stress-strength reliability metric $\mathcal{R}$ from Group–A (or Group–B) is considered to be $\frac{1}{3}$. The simulation framework incorporates various progressive censoring schemes, denoted by **R** and **Q**, along with different combinations of sample sizes $(n_i,\ i = 1, 2)$, effective sample counts $(m_i,\ i = 1, 2)$, and termination times ($T_i^{\min}$ and $T_i^{\max}$) for $i = 1, 2$, all of which are systematically organized in Table 1. For each setup in Table 1, two thresholds ($\{(T_1^{\min}, T_1^{\max}), (T_2^{\min}, T_2^{\max})\}$) are utilized. namely {(0.3,0.8),(0.5.1.2)} and {(0.5,1.0),(0.8.1.5)} (for Group–A) and {(0.4,0.6),(0.6.0.8)} and {(0.6,0.8),(0.8.0.9)} (for Group–B). Four distinct PT2C strategies labeled as CS[i] (for i=1,2,3,4) are employed to facilitate comparison. These represent uniform, left, center, middle, and right censoring configurations. In this table, for distinction, the censoring pattern $\{(1^\star 20), (1^\star 15)\}$ represents (for example) one survival item that will be uniformly drawn from the life test 20 (15) times in Group–A (Group–B).

Table 1. Several PT2C scenarios for comparison in Monte Carlo investigations.

(n_1, m_1)	(n_2, m_2)	Test	$\{\underline{R}, \underline{Q}\}$
(40,20)	(30,15)	I	CS[1]:{(1*20),(1*15)}
		II	CS[2]:{(5*4,0*16),(5*3,0*12)}
		III	CS[3]:{(0*8,5*4,0*8),(0*6,5*3,0*6)}
		IV	CS[4]:(0*16,5*4),(0*12,5*3)}
(40,30)	(30,25)	I	CS[1]:{(1*10,0*20),(1*5,0*20)}
		II	CS[2]:{(5*2,0*28),(5*1,0*24)}
		III	CS[3]:{(0*14,5*2,0*14),(0*12,5*1,0*12)}
		IV	CS[4]:(0*28,5*2),(0*24,5*1)}
(60,30)	(80,40)	I	CS[1]:{(1*30),(1*40)}
		II	CS[2]:{(5*6,0*24),(5*8,0*32)}
		III	CS[3]:{(0*12,5*6,0*12),(0*16,5*8,0*16)}
		IV	CS[4]:(0*24,5*6),(0*32,5*8)}
(60,50)	(80,60)	I	CS[1]:{(1*10,0*40),(1*20,0*40)}
		II	CS[2]:{(5*2,0*48),(5*4,0*56)}
		III	CS[3]:{(0*24,5*2,0*24),(0*28,5*4,0*28)}
		IV	CS[4]:(0*48,5*2),(0*56,5*4)}

To generate an IAPT2C sample, beyond assigning the counts of m_i, n_i, $T_i^{\min}$, and $T_i^{\max}$ (for $i = 1, 2$), and the progressive censoring scheme $\{\mathbf{R}, \mathbf{Q}\}$, follow the procedure outlined below:

Step 1: Specify the true values of the Weibull(θ_1, δ) population model.

Step 2: Generate a traditional PT2C sample as follows:

(a) Simulate ζ independent random variables $\zeta_1, \zeta_2, \ldots, \zeta_{m_1}$ from uniform $U(0, 1)$ distribution.
(b) Compute $\Lambda_i = \zeta_i^{\left(i+\sum_{j=m_1-i+1}^{m_1} R_j\right)^{-1}}$ for $i = 1, 2, \ldots, m_1$.
(c) Obtain $U_i = 1 - \prod_{k=m_1-i+1}^{m_1} \Lambda_k$ for $i = 1, 2, \ldots, m_1$.
(d) Generate a PT2C sample of size m_1 from the Weibull(θ_1, δ) distribution using the inversion method:

$$X_i = \left[-\frac{1}{\theta_1}\log\left(1 - \log(u_i)\right)\right]^{\frac{1}{\delta}}, \quad i = 1, 2, \ldots, m_1.$$

Step 3: Identify the truncation point r_1 corresponding to the predetermined threshold $T_1^{\min}$, then discard the remaining observations $X_{r_1+2}, \ldots, X_{m_1}$.

Step 4. Find the first $m_1 - r_1 - 1$ order statistics (say $X_{r_1+2}, \ldots, X_{m_1}$) from a truncated distribution $g(x)\left[1 - G\left(x_{r_1+1}\right)\right]^{-1}$ with sample size $n - r_1 - 1 - \sum_{i=1}^{r_1} R_i$.

Step 5. Find the IAPT2C data type as:

a. Case-1: If $X_{m_1} < T_1^{\min} < T_1^{\max}$; stop the test at X_{m_1}.

b. Case-2: If $T_1^{\min} < X_{m_1} < T_1^{\max}$; stop the test at X_{m_1}.
c. Case-3: If $T_1^{\min} < T_1^{\max} < X_{m_1}$; stop the test at T_2.

Step 6: Repeat Steps 1–5 for the Weibull(θ_2, δ) population to generate the second sample.

After generating 1,000 IAPT2C samples, to calculate the offered point and interval estimators of $\theta_i,\ i = 1, 2,\ \delta$, and $\mathcal{R}$, we proceed with the analysis using two widely adopted packages in R programming environment (version 4.2.2):

- The maxLik package, developed by Henningsen and Toomet [29], is utilized to compute the ML/MPS estimates and associated $100\%(1-\alpha)$ ACI-LF/ACI-SF estimates under the frequentist paradigm.
- The coda package, by Plummer et al. [30], facilitates the Bayesian analysis by providing tools for MCMC diagnostics and posterior summaries for the same unknown subjects.

A central challenge in Bayesian inference lies in the selection of appropriate hyper-parameters. In this study, we adopt a data-informed approach to determine the hyper-parameters λ_i and β_i for $i = 1, 2$ in the joint gamma prior assigned to $\theta_i,\ i = 1, 2$, based on synthetic historical data. Specifically, 10,000 past complete samples are simulated under the condition $n_i = 50$ (for instance). Firstly, without loss of generality, we fix (λ_3, β_3) = (1,2) and (3,2) for Group–A and Group–B, respectively, for the parameter δ. We follow the past samples algorithm discussed in Nassar and Elshahhat [21], the hyper-parameter values $(\lambda_1, \lambda_2, \beta_1, \beta_2)$ of $\theta_i,\ i = 1, 2$, such as

- (75.7121, 79.5140, 184.228, 96.8975) and (73.9323, 71.9484, 169.421, 82.4678) from ML and MPS functions, respectively, at Group–A;
- (75.7139, 77.8583, 73.6933, 37.8260) and (73.0303, 75.6225, 67.0839, 34.7833) from ML and MPS functions, respectively, at Group–B.

To implement the MCMC algorithm described in Section 4, we generate 12,000 iterations, discarding the initial 2,000 as burn-in to mitigate the influence of initial values. Subsequently, from 10,000 MCMC iterations developed from LFBA and SFBA methodologies, the Bayesian estimates, along with corresponding BCI estimates for $\theta_i,\ i = 1, 2,\ \delta$, and the stress-strength reliability measure $\mathcal{R}$, are computed.

Specifically, the average point estimate (APE) of $\mathcal{R}$ (as an example) is computed as

$$\text{APE}(\breve{\mathcal{R}}) = \frac{1}{1000}\sum_{j=1}^{1000}\breve{\mathcal{R}}^{[j]},$$

where $\breve{\mathcal{R}}^{[j]}$ denotes the computed point estimate of $\mathcal{R}$ at ith simulated sample.

Next, two metrics of point assessments, namely root mean squared error (RMSE) and average relative absolute bias (ARAB), are performed to see the superiority of $\mathcal{R}$, respectively, as

$$\text{RMSE}(\breve{\mathcal{R}}) = \sqrt{\frac{1}{1000}\sum_{j=1}^{1000}\left(\breve{\mathcal{R}}^{[j]} - \mathcal{R}\right)^2},$$

and

$$\text{ARAB}(\breve{\mathcal{R}}) = \frac{1}{1000}\sum_{j=1}^{1000}\mathcal{R}^{-1}\left|\breve{\mathcal{R}}^{[j]} - \mathcal{R}\right|.$$

On the other hand, two metrics of interval assessments, namely average interval length (AIL) and coverage percentage (CP) are also considered as

$$\mathrm{AIL}_{(1-\alpha)\%}(\mathcal{R}) = \frac{1}{1000}\sum\nolimits_{j=1}^{1000}\left(\mathcal{U}_{\check{\mathcal{R}}[j]} - \mathcal{L}_{\check{\mathcal{R}}[j]}\right)$$

and

$$\mathrm{CP}_{(1-\alpha)\%}(\mathcal{R}) = \frac{1}{1000}\sum_{j=1}^{1000}\mathbf{J}^{\bullet}{}_{\left(\mathbb{L}_{\check{\mathcal{R}}[j]};\mathbb{U}_{\check{\mathcal{R}}[j]}\right)}(\mathcal{R}),$$

respectively, where $\mathbf{J}^{\bullet}(\cdot)$ is the indicator function and $(\mathbb{L}(\cdot), \mathbb{U}(\cdot))$ denotes the (lower,upper) sides of the $(1-\alpha)\%$ ACI (or BCI) estimate of $\mathcal{R}$.

Part of the simulation results for $\theta_i, \imath = 1, 2$, δ, and $\mathcal{R}$ when $n = 40$ are reported in Tables 2–5, and other results when $n = 60$ are available as supplementary material, for brevity. Tables 2–5 present the RMSEs (first column) and ARABs (second column), while Tables 6–9 display the AILs (first column) and CP (second column), all evaluated at the $\alpha = 5\%$ significance level. Based on the performance metrics reported in Tables 2–9, in terms of the lowest RMSE, ARAB, and AIL values, as well as the highest CP values, we summarize the following key findings:

- In general, all estimators of $\theta_i,\ i = 1, 2$, δ, and $\mathcal{R}$ derived using the proposed estimation procedures perform reliably and with satisfactory precision.
- When n_i (or m_i) increases (for $i = 1, 2$), the estimation accuracy improves. A similar improvement is observed when the total number of censored units, $\sum_{i=1}^{m_1} R_i$ or $\sum_{i=1}^{m_2} Q_i$, is reduced.
- Increasing the pre-specified test durations $T_i^{\min}$ and $T_i^{\max}$ $(i = 1, 2)$ generally leads to reductions in RMSE, ARAB, and AIL values across all parameters, with an improvement in CP levels, indicating higher precision and reliability of the resulting estimators. Thus, to obtain high-quality estimates of unknown lifetime parameters under progressive censoring, practitioners are encouraged to maximize the test duration within feasible cost constraints.
- Owing to the incorporation of informative gamma priors, the Bayesian MCMC estimates created from LFBA (or SFBA) for $\theta_i,\ i = 1, 2$, δ, and $\mathcal{R}$ consistently outperform their frequentist counterparts. This advantage extends to interval estimation, where credible intervals yield narrower AILs and higher CPs compared to ACIs.
- A comparison of point and interval estimation strategies reveals the following:
  - The ML method outperformed the MPS method for $\theta_i,\ i = 1, 2$, and δ, while the opposite case is noted for the stress-strength reliability measure $\mathcal{R}$;
  - The LFBA method outperformed the SFBA method for $\theta_i,\ i = 1, 2$, and δ, while the opposite case for $\mathcal{R}$;
  - The ACI method through LF outperformed its competitor, the ACI method through SF, for $\theta_i,\ i = 1, 2$, and δ, while the ACI method through SF outperformed the ACI method through LF for $\mathcal{R}$;
  - The BCI method through SFBA outperformed its competitors through LFBA for $\mathcal{R}$, while the BCI method through LFBA outperformed its competitors through SFBA for $\theta_i,\ i = 1, 2$, and δ.

- Comparing the suggested PT2C strategies, it is noted that:
  - The estimates of $\theta_i,\ i = 1, 2$ exhibit superior behavior under CS[4] "right censoring";
  - The estimates of δ exhibit superior behavior under CS[1] "uniform censoring."
- As $\theta_i,\ i = 1, 2$, and δ increase, it is noted that:
  - The RMSEs and ARABs of θ_1 and $\mathcal{R}$ decrease while those of θ_2 and δ increase;
  - The RMSEs and ARABs of θ_1 and $\mathcal{R}$ decrease while those of θ_2 and δ increase;
  - The AIL values for ACIs of θ_1 increase while those of BCI decrease. The CP values for ACIs of θ_1 decrease while those of BCIs increase;
  - The AIL values of θ_2 and δ increase, except their CP values decrease;
  - The AIL values of $\mathcal{R}$ decrease except their CP values increase.
- In conclusion, for data generated under the proposed IAPT2C sampling design, the MCMC approach using SFBA-based is recommended for analyzing the Weibull stress-strength reliability index.

Table 2. Point assessments of θ_1.

(n_1, m_1)	(n_2, m_2)	Test	MLE			MPSE			MCMC[LFBA]			MCMC[SFBA]		
Group–A→			$\{(T_1^{\min}, T_1^{\max}), (T_2^{\min}, T_2^{\max})\}$={(0.3,0.8),(0.5.1.2)}											
(40,20)	(30,15)	I	0.427	0.371	0.864	0.455	0.423	0.966	0.733	0.146	0.255	0.786	0.180	0.304
		II	0.417	0.362	0.835	0.442	0.420	0.959	0.730	0.135	0.241	0.780	0.160	0.281
		III	0.433	0.363	0.845	0.468	0.422	0.963	0.725	0.139	0.243	0.785	0.167	0.287
		IV	0.428	0.362	0.835	0.457	0.417	0.951	0.732	0.134	0.240	0.783	0.159	0.277
(40,30)	(30,25)	I	0.439	0.354	0.832	0.470	0.360	0.838	0.738	0.130	0.239	0.690	0.158	0.276
		II	0.439	0.328	0.768	0.470	0.358	0.826	0.734	0.117	0.218	0.683	0.140	0.253
		III	0.444	0.352	0.830	0.482	0.358	0.833	0.746	0.118	0.226	0.693	0.145	0.258
		IV	0.444	0.323	0.734	0.475	0.355	0.814	0.734	0.112	0.215	0.683	0.129	0.238
Group–A→			$\{(T_1^{\min}, T_1^{\max}), (T_2^{\min}, T_2^{\max})\}$={(0.5,1.0),(0.8.1.5)}											
(40,20)	(30,15)	I	0.418	0.364	0.849	0.443	0.420	0.960	0.726	0.141	0.226	0.784	0.146	0.264
		II	0.416	0.355	0.823	0.440	0.416	0.949	0.723	0.134	0.221	0.780	0.138	0.251
		III	0.426	0.361	0.838	0.457	0.418	0.949	0.720	0.137	0.225	0.780	0.140	0.262
		IV	0.410	0.353	0.817	0.437	0.407	0.929	0.716	0.132	0.218	0.771	0.137	0.248
(40,30)	(30,25)	I	0.432	0.351	0.816	0.460	0.365	0.830	0.735	0.127	0.209	0.686	0.131	0.236
		II	0.427	0.326	0.764	0.453	0.349	0.801	0.729	0.122	0.204	0.678	0.122	0.228
		III	0.434	0.350	0.806	0.467	0.350	0.827	0.739	0.124	0.204	0.689	0.129	0.232
		IV	0.435	0.318	0.732	0.463	0.344	0.789	0.727	0.120	0.203	0.676	0.121	0.224
Group–B→			$\{(T_1^{\min}, T_1^{\max}), (T_2^{\min}, T_2^{\max})\}$={(0.4,0.6),(0.6.0.8)}											
(40,20)	(30,15)	I	1.053	0.318	0.262	1.122	0.393	0.274	1.211	0.254	0.214	1.264	0.290	0.230
		II	1.031	0.308	0.238	1.094	0.362	0.268	1.210	0.241	0.201	1.262	0.261	0.221
		III	1.075	0.310	0.239	1.161	0.376	0.269	1.206	0.242	0.210	1.262	0.274	0.226
		IV	1.058	0.300	0.238	1.133	0.355	0.267	1.212	0.236	0.193	1.263	0.259	0.220
(40,30)	(30,25)	I	1.087	0.294	0.237	1.162	0.348	0.266	1.235	0.217	0.150	1.148	0.258	0.216
		II	1.084	0.270	0.229	1.156	0.309	0.252	1.232	0.187	0.148	1.146	0.255	0.213
		III	1.095	0.297	0.236	1.187	0.333	0.253	1.235	0.207	0.148	1.149	0.257	0.216
		IV	1.099	0.259	0.219	1.173	0.298	0.246	1.234	0.177	0.147	1.147	0.245	0.213
Group–B→			$\{(T_1^{\min}, T_1^{\max}), (T_2^{\min}, T_2^{\max})\}$={(0.6,0.8),(0.8.0.9)}											
(40,20)	(30,15)	I	1.041	0.303	0.237	1.100	0.333	0.266	1.205	0.264	0.204	1.262	0.283	0.234
		II	1.055	0.294	0.234	1.115	0.310	0.263	1.206	0.253	0.195	1.262	0.268	0.220
		III	1.056	0.297	0.236	1.126	0.311	0.265	1.203	0.256	0.200	1.258	0.273	0.232
		IV	1.020	0.290	0.233	1.090	0.307	0.260	1.204	0.245	0.194	1.255	0.264	0.219
(40,30)	(30,25)	I	1.069	0.262	0.214	1.129	0.299	0.223	1.233	0.236	0.191	1.145	0.237	0.214
		II	1.063	0.241	0.206	1.121	0.277	0.213	1.230	0.207	0.184	1.142	0.234	0.190
		III	1.070	0.248	0.214	1.143	0.285	0.220	1.234	0.223	0.190	1.148	0.235	0.213
		IV	1.073	0.234	0.200	1.132	0.274	0.212	1.230	0.202	0.180	1.145	0.233	0.185

Table 3. Point assessments of θ_2.

(n_1, m_1)	(n_2, m_2)	Test	MLE			MPSE			MCMC[LFBA]			MCMC[SFBA]		
Group–A→			$\{(T_1^{\min}, T_1^{\max}), (T_2^{\min}, T_2^{\max})\}$={(0.3,0.8),(0.5.1.2)}											
(40,20)	(30,15)	I	0.893	0.314	0.353	1.006	0.398	0.365	0.938	0.300	0.270	0.964	0.307	0.336
		II	0.844	0.297	0.294	0.919	0.368	0.317	0.944	0.230	0.258	0.966	0.259	0.263
		III	0.874	0.315	0.361	0.959	0.459	0.365	0.935	0.310	0.277	0.960	0.309	0.356
		IV	0.856	0.295	0.287	0.942	0.365	0.313	0.940	0.228	0.256	0.962	0.254	0.262
(40,30)	(30,25)	I	0.888	0.261	0.244	0.985	0.354	0.304	0.953	0.183	0.195	0.913	0.203	0.220
		II	0.886	0.250	0.234	0.964	0.340	0.287	0.956	0.180	0.191	0.920	0.194	0.208
		III	0.882	0.287	0.262	0.963	0.357	0.313	0.953	0.191	0.195	0.916	0.204	0.220
		IV	0.892	0.243	0.229	0.972	0.320	0.268	0.956	0.179	0.187	0.920	0.192	0.207
Group–A→			$\{(T_1^{\min}, T_1^{\max}), (T_2^{\min}, T_2^{\max})\}$={(0.5,1.0),(0.8.1.5)}											
(40,20)	(30,15)	I	0.850	0.294	0.340	0.924	0.323	0.376	0.938	0.216	0.211	0.962	0.250	0.233
		II	0.819	0.240	0.267	0.873	0.244	0.277	0.942	0.211	0.202	0.963	0.237	0.225
		III	0.812	0.298	0.344	0.868	0.326	0.379	0.944	0.228	0.220	0.965	0.274	0.258
		IV	0.792	0.235	0.256	0.861	0.238	0.271	0.940	0.199	0.192	0.965	0.224	0.212
(40,30)	(30,25)	I	0.839	0.207	0.203	0.899	0.213	0.224	0.954	0.180	0.184	0.918	0.191	0.193
		II	0.823	0.200	0.203	0.872	0.211	0.217	0.951	0.179	0.182	0.914	0.184	0.190
		III	0.838	0.214	0.211	0.893	0.223	0.231	0.954	0.180	0.189	0.919	0.197	0.198
		IV	0.837	0.182	0.201	0.888	0.209	0.206	0.952	0.178	0.181	0.913	0.181	0.189
Group–B→			$\{(T_1^{\min}, T_1^{\max}), (T_2^{\min}, T_2^{\max})\}$={(0.4,0.6),(0.6.0.8)}											
(40,20)	(30,15)	I	2.240	0.722	0.256	2.535	0.989	0.334	1.989	0.203	0.085	2.045	0.246	0.092
		II	2.154	0.717	0.251	2.364	0.928	0.315	1.990	0.148	0.064	2.046	0.169	0.063
		III	2.213	0.728	0.262	2.445	1.037	0.356	1.990	0.210	0.092	2.045	0.262	0.098
		IV	2.171	0.705	0.247	2.404	0.920	0.309	1.993	0.141	0.064	2.046	0.177	0.060
(40,30)	(30,25)	I	2.236	0.671	0.245	2.494	0.899	0.308	2.014	0.119	0.037	1.983	0.139	0.043
		II	2.230	0.668	0.241	2.440	0.890	0.307	2.015	0.109	0.033	1.986	0.134	0.040
		III	2.220	0.689	0.247	2.439	0.911	0.309	2.015	0.129	0.045	1.983	0.143	0.057
		IV	2.251	0.645	0.231	2.467	0.874	0.285	2.015	0.094	0.030	1.986	0.123	0.039
Group–B→			$\{(T_1^{\min}, T_1^{\max}), (T_2^{\min}, T_2^{\max})\}$={(0.6,0.8),(0.8.0.9)}											
(40,20)	(30,15)	I	2.169	0.616	0.221	2.400	0.800	0.268	1.990	0.170	0.086	2.043	0.186	0.078
		II	2.171	0.611	0.217	2.358	0.791	0.267	1.989	0.166	0.063	2.047	0.170	0.065
		III	2.129	0.625	0.229	2.315	0.841	0.292	1.989	0.172	0.089	2.046	0.196	0.099
		IV	2.110	0.597	0.216	2.324	0.769	0.261	1.992	0.154	0.059	2.040	0.168	0.064
(40,30)	(30,25)	I	2.149	0.592	0.211	2.341	0.741	0.251	2.013	0.132	0.047	1.981	0.140	0.051
		II	2.148	0.580	0.209	2.310	0.735	0.247	2.013	0.128	0.043	1.983	0.132	0.048
		III	2.149	0.592	0.213	2.318	0.750	0.255	2.014	0.138	0.053	1.984	0.143	0.058
		IV	2.151	0.563	0.207	2.313	0.730	0.247	2.013	0.125	0.036	1.984	0.131	0.044

Table 4. Point assessments of δ.

(n_1, m_1)	(n_2, m_2)	Test	MLE			MPSE			MCMC[LFBA]			MCMC[SFBA]		
Group–A→			$\{(T_1^{\min}, T_1^{\max}), (T_2^{\min}, T_2^{\max})\}$={(0.3,0.8),(0.5.1.2)}											
(40,20)	(30,15)	I	0.461	0.115	0.184	0.434	0.132	0.206	0.457	0.097	0.156	0.508	0.112	0.161
		II	0.502	0.134	0.206	0.450	0.137	0.222	0.483	0.111	0.166	0.530	0.128	0.182
		III	0.471	0.141	0.218	0.435	0.143	0.226	0.468	0.115	0.183	0.516	0.130	0.184
		IV	0.472	0.124	0.200	0.436	0.136	0.215	0.464	0.100	0.158	0.510	0.119	0.164
(40,30)	(30,25)	I	0.478	0.100	0.144	0.445	0.102	0.160	0.613	0.086	0.114	0.578	0.096	0.138
		II	0.490	0.110	0.152	0.448	0.112	0.180	0.603	0.093	0.127	0.569	0.104	0.150
		III	0.488	0.111	0.158	0.450	0.115	0.180	0.608	0.097	0.130	0.575	0.108	0.155
		IV	0.475	0.100	0.148	0.442	0.107	0.173	0.613	0.089	0.119	0.578	0.098	0.144
Group–A→			$\{(T_1^{\min}, T_1^{\max}), (T_2^{\min}, T_2^{\max})\}$={(0.5,1.0),(0.8.1.5)}											
(40,20)	(30,15)	I	0.505	0.116	0.188	0.486	0.125	0.188	0.464	0.101	0.166	0.502	0.111	0.167
		II	0.494	0.136	0.214	0.445	0.142	0.215	0.477	0.112	0.180	0.519	0.124	0.185
		III	0.473	0.153	0.230	0.439	0.167	0.252	0.475	0.142	0.207	0.517	0.147	0.222
		IV	0.489	0.130	0.200	0.455	0.139	0.202	0.473	0.107	0.167	0.513	0.124	0.179
(40,30)	(30,25)	I	0.473	0.102	0.149	0.442	0.102	0.166	0.594	0.085	0.114	0.570	0.095	0.137
		II	0.482	0.107	0.155	0.442	0.107	0.176	0.608	0.091	0.128	0.578	0.107	0.146
		III	0.483	0.111	0.163	0.447	0.114	0.182	0.615	0.092	0.130	0.580	0.108	0.148
		IV	0.472	0.104	0.151	0.439	0.106	0.170	0.601	0.090	0.126	0.571	0.101	0.144
Group–B→			$\{(T_1^{\min}, T_1^{\max}), (T_2^{\min}, T_2^{\max})\}$={(0.4,0.6),(0.6.0.8)}											
(40,20)	(30,15)	I	0.765	0.196	0.189	0.755	0.199	0.194	0.793	0.184	0.121	0.839	0.193	0.145
		II	0.844	0.205	0.217	0.799	0.221	0.228	0.799	0.200	0.128	0.843	0.204	0.155
		III	0.779	0.221	0.223	0.750	0.230	0.235	0.796	0.206	0.136	0.840	0.211	0.161
		IV	0.776	0.200	0.202	0.746	0.210	0.220	0.799	0.184	0.125	0.842	0.199	0.147
(40,30)	(30,25)	I	0.803	0.169	0.163	0.780	0.184	0.173	0.917	0.158	0.063	0.891	0.168	0.108
		II	0.822	0.191	0.177	0.792	0.196	0.191	0.916	0.166	0.106	0.888	0.173	0.126
		III	0.818	0.192	0.184	0.788	0.197	0.192	0.916	0.175	0.120	0.887	0.191	0.134
		IV	0.793	0.170	0.168	0.767	0.185	0.181	0.917	0.160	0.105	0.889	0.170	0.112
Group–B→			$\{(T_1^{\min}, T_1^{\max}), (T_2^{\min}, T_2^{\max})\}$={(0.6,0.8),(0.8.0.9)}											
(40,20)	(30,15)	I	0.849	0.207	0.164	0.852	0.210	0.179	0.792	0.168	0.127	0.828	0.181	0.144
		II	0.838	0.221	0.206	0.788	0.222	0.216	0.794	0.212	0.128	0.833	0.219	0.148
		III	0.805	0.265	0.227	0.774	0.324	0.237	0.805	0.220	0.131	0.844	0.230	0.150
		IV	0.845	0.211	0.203	0.816	0.213	0.211	0.816	0.204	0.128	0.852	0.211	0.146
(40,30)	(30,25)	I	0.798	0.172	0.147	0.770	0.186	0.150	0.916	0.149	0.070	0.890	0.152	0.119
		II	0.807	0.193	0.154	0.769	0.199	0.162	0.920	0.157	0.114	0.893	0.165	0.124
		III	0.811	0.194	0.155	0.776	0.199	0.165	0.918	0.159	0.122	0.892	0.166	0.126
		IV	0.805	0.173	0.151	0.775	0.189	0.161	0.917	0.154	0.070	0.892	0.161	0.124

Table 5. Point assessments of $\mathcal{R}$.

(n_1, m_1)	(n_2, m_2)	Test	MLE			MPSE			MCMC[LFBA]			MCMC[SFBA]		
Group–A→			$\{(T_1^{\min}, T_1^{\max}), (T_2^{\min}, T_2^{\max})\}$={(0.3,0.8),(0.5.1.2)}											
(40,20)	(30,15)	I	0.339	0.112	0.324	0.335	0.104	0.309	0.434	0.090	0.217	0.444	0.088	0.211
		II	0.335	0.118	0.331	0.328	0.107	0.327	0.433	0.094	0.224	0.444	0.091	0.218
		III	0.337	0.116	0.325	0.333	0.106	0.311	0.433	0.090	0.221	0.442	0.088	0.213
		IV	0.335	0.122	0.336	0.330	0.111	0.331	0.436	0.095	0.231	0.445	0.091	0.222
(40,30)	(30,25)	I	0.340	0.102	0.294	0.337	0.094	0.268	0.431	0.087	0.211	0.423	0.081	0.203
		II	0.340	0.104	0.298	0.337	0.098	0.278	0.436	0.089	0.215	0.428	0.085	0.208
		III	0.339	0.102	0.294	0.336	0.094	0.268	0.431	0.088	0.214	0.423	0.084	0.204
		IV	0.339	0.108	0.300	0.336	0.100	0.283	0.433	0.089	0.217	0.426	0.088	0.211
Group–A→			$\{(T_1^{\min}, T_1^{\max}), (T_2^{\min}, T_2^{\max})\}$={(0.5,1.0),(0.8.1.5)}											
(40,20)	(30,15)	I	0.345	0.113	0.318	0.341	0.102	0.291	0.429	0.078	0.187	0.439	0.077	0.185
		II	0.338	0.122	0.327	0.335	0.106	0.297	0.431	0.081	0.193	0.442	0.080	0.191
		III	0.341	0.116	0.326	0.339	0.103	0.296	0.431	0.079	0.190	0.442	0.079	0.188
		IV	0.343	0.127	0.329	0.341	0.110	0.301	0.431	0.085	0.203	0.443	0.083	0.200
(40,30)	(30,25)	I	0.345	0.097	0.289	0.345	0.094	0.266	0.430	0.075	0.179	0.422	0.073	0.175
		II	0.345	0.102	0.293	0.345	0.096	0.272	0.434	0.076	0.181	0.425	0.076	0.181
		III	0.344	0.101	0.290	0.344	0.094	0.268	0.431	0.075	0.180	0.423	0.075	0.180
		IV	0.344	0.107	0.294	0.343	0.097	0.275	0.432	0.077	0.185	0.424	0.076	0.183
Group–B→			$\{(T_1^{\min}, T_1^{\max}), (T_2^{\min}, T_2^{\max})\}$={(0.4,0.6),(0.6.0.8)}											
(40,20)	(30,15)	I	0.335	0.080	0.184	0.330	0.076	0.163	0.377	0.051	0.132	0.381	0.048	0.117
		II	0.331	0.083	0.201	0.323	0.080	0.191	0.377	0.053	0.138	0.380	0.051	0.128
		III	0.330	0.082	0.194	0.325	0.078	0.188	0.377	0.052	0.135	0.381	0.049	0.124
		IV	0.329	0.087	0.207	0.323	0.083	0.197	0.378	0.058	0.139	0.381	0.052	0.134
(40,30)	(30,25)	I	0.334	0.073	0.151	0.330	0.069	0.141	0.379	0.039	0.112	0.366	0.037	0.098
		II	0.335	0.078	0.163	0.330	0.073	0.151	0.380	0.044	0.121	0.367	0.040	0.100
		III	0.333	0.077	0.155	0.329	0.071	0.146	0.379	0.042	0.118	0.366	0.039	0.099
		IV	0.335	0.078	0.168	0.330	0.075	0.158	0.379	0.047	0.127	0.366	0.044	0.111
Group–B→			$\{(T_1^{\min}, T_1^{\max}), (T_2^{\min}, T_2^{\max})\}$={(0.6,0.8),(0.8.0.9)}											
(40,20)	(30,15)	I	0.332	0.037	0.175	0.327	0.048	0.165	0.376	0.073	0.139	0.380	0.074	0.136
		II	0.333	0.049	0.181	0.327	0.054	0.174	0.376	0.076	0.148	0.380	0.077	0.138
		III	0.332	0.048	0.180	0.327	0.050	0.168	0.377	0.075	0.140	0.380	0.075	0.137
		IV	0.334	0.055	0.190	0.328	0.056	0.183	0.377	0.079	0.151	0.380	0.081	0.144
(40,30)	(30,25)	I	0.338	0.039	0.168	0.334	0.042	0.133	0.379	0.067	0.122	0.366	0.070	0.097
		II	0.338	0.040	0.172	0.335	0.044	0.151	0.379	0.070	0.130	0.367	0.072	0.110
		III	0.336	0.036	0.171	0.333	0.042	0.147	0.379	0.069	0.128	0.365	0.071	0.098
		IV	0.338	0.046	0.173	0.334	0.046	0.156	0.379	0.072	0.133	0.366	0.073	0.121

Table 6. Interval assessments of θ_1.

(n_1, m_1)	(n_2, m_2)	Test	ACI				BCI			
			LF		SF		LFBA		SFBA	
Group–A→			$\{(T_1^{\min}, T_1^{\max}), (T_2^{\min}, T_2^{\max})\}$={(0.3,0.8),(0.5.1.2)}							
(40,20)	(30,15)	I	0.541	0.923	0.548	0.920	0.458	0.923	0.466	0.925
		II	0.504	0.924	0.534	0.925	0.445	0.925	0.447	0.928
		III	0.538	0.924	0.541	0.920	0.449	0.925	0.461	0.926
		IV	0.486	0.926	0.527	0.928	0.431	0.928	0.442	0.929
(40,30)	(30,25)	I	0.441	0.932	0.484	0.935	0.430	0.928	0.431	0.931
		II	0.440	0.933	0.479	0.935	0.410	0.931	0.427	0.931
		III	0.440	0.932	0.484	0.935	0.424	0.929	0.430	0.931
		IV	0.422	0.939	0.438	0.937	0.379	0.936	0.410	0.934
Group–A→			$\{(T_1^{\min}, T_1^{\max}), (T_2^{\min}, T_2^{\max})\}$={(0.5,1.0),(0.8.1.5)}							
(40,20)	(30,15)	I	0.502	0.925	0.542	0.925	0.332	0.938	0.449	0.927
		II	0.458	0.926	0.537	0.931	0.338	0.937	0.443	0.928
		III	0.483	0.925	0.541	0.928	0.337	0.937	0.448	0.928
		IV	0.452	0.927	0.527	0.932	0.344	0.936	0.436	0.930
(40,30)	(30,25)	I	0.433	0.938	0.445	0.935	0.347	0.935	0.422	0.932
		II	0.428	0.940	0.434	0.936	0.355	0.934	0.399	0.936
		III	0.430	0.940	0.436	0.936	0.348	0.935	0.415	0.933
		IV	0.422	0.941	0.428	0.937	0.374	0.930	0.395	0.936
Group–B→			$\{(T_1^{\min}, T_1^{\max}), (T_2^{\min}, T_2^{\max})\}$={(0.4,0.6),(0.6.0.8)}							
(40,20)	(30,15)	I	1.061	0.921	1.234	0.925	0.381	0.915	0.463	0.916
		II	1.003	0.928	1.122	0.929	0.378	0.915	0.459	0.917
		III	1.039	0.924	1.191	0.927	0.380	0.915	0.461	0.917
		IV	0.983	0.930	1.093	0.931	0.372	0.917	0.456	0.917
(40,30)	(30,25)	I	0.977	0.931	1.084	0.931	0.320	0.928	0.363	0.934
		II	0.976	0.931	1.082	0.931	0.270	0.940	0.361	0.935
		III	0.977	0.931	1.083	0.931	0.316	0.930	0.361	0.935
		IV	0.976	0.934	1.038	0.931	0.268	0.940	0.358	0.935
Group–B→			$\{(T_1^{\min}, T_1^{\max}), (T_2^{\min}, T_2^{\max})\}$={(0.6,0.8),(0.8.0.9)}							
(40,20)	(30,15)	I	0.970	0.922	1.101	0.926	0.372	0.915	0.456	0.916
		II	0.932	0.928	1.024	0.929	0.368	0.916	0.454	0.916
		III	0.942	0.926	1.054	0.928	0.371	0.915	0.454	0.916
		IV	0.913	0.929	1.002	0.930	0.365	0.916	0.451	0.917
(40,30)	(30,25)	I	0.899	0.930	0.990	0.931	0.303	0.931	0.358	0.934
		II	0.876	0.933	0.954	0.933	0.266	0.939	0.354	0.935
		III	0.889	0.932	0.968	0.932	0.302	0.931	0.358	0.934
		IV	0.857	0.934	0.939	0.934	0.262	0.940	0.353	0.935

Table 7. Interval assessments of θ_2.

(n_1, m_1)	(n_2, m_2)	Test	ACI				BCI			
			LF		SF		LFBA		SFBA	
Group–A→			$\{(T_1^{\min}, T_1^{\max}), (T_2^{\min}, T_2^{\max})\}$={(0.3,0.8),(0.5.1.2)}							
(40,20)	(30,15)	I	1.018	0.918	1.233	0.913	0.384	0.917	0.414	0.919
		II	0.995	0.920	1.176	0.917	0.373	0.918	0.409	0.921
		III	1.075	0.913	1.367	0.903	0.412	0.914	0.426	0.913
		IV	0.986	0.920	1.168	0.917	0.322	0.929	0.353	0.932
(40,30)	(30,25)	I	0.973	0.921	1.131	0.920	0.309	0.936	0.318	0.935
		II	0.973	0.921	1.130	0.920	0.299	0.937	0.313	0.937
		III	0.980	0.921	1.150	0.919	0.316	0.934	0.329	0.933
		IV	0.779	0.937	0.874	0.938	0.299	0.940	0.301	0.937
Group–A→			$\{(T_1^{\min}, T_1^{\max}), (T_2^{\min}, T_2^{\max})\}$={(0.5,1.0),(0.8.1.5)}							
(40,20)	(30,15)	I	0.860	0.918	0.969	0.916	0.381	0.915	0.425	0.919
		II	0.825	0.922	0.933	0.919	0.376	0.917	0.416	0.920
		III	0.908	0.914	1.070	0.907	0.438	0.908	0.463	0.907
		IV	0.817	0.922	0.923	0.920	0.327	0.933	0.338	0.931
(40,30)	(30,25)	I	0.782	0.926	0.874	0.924	0.305	0.939	0.305	0.936
		II	0.779	0.926	0.864	0.925	0.301	0.940	0.303	0.936
		III	0.815	0.923	0.910	0.921	0.313	0.933	0.335	0.934
		IV	0.776	0.926	0.857	0.926	0.290	0.940	0.299	0.939
Group–B→			$\{(T_1^{\min}, T_1^{\max}), (T_2^{\min}, T_2^{\max})\}$={(0.4,0.6),(0.6.0.8)}							
(40,20)	(30,15)	I	2.401	0.919	2.810	0.916	0.410	0.912	0.456	0.938
		II	2.369	0.920	2.717	0.919	0.339	0.928	0.375	0.949
		III	2.482	0.916	3.082	0.908	0.411	0.912	0.457	0.938
		IV	2.318	0.922	2.677	0.920	0.338	0.929	0.371	0.949
(40,30)	(30,25)	I	2.303	0.922	2.620	0.921	0.284	0.930	0.364	0.957
		II	2.261	0.924	2.590	0.922	0.282	0.943	0.298	0.957
		III	2.308	0.922	2.669	0.920	0.285	0.929	0.369	0.957
		IV	2.258	0.924	2.585	0.922	0.281	0.943	0.297	0.958
Group–B→			$\{(T_1^{\min}, T_1^{\max}), (T_2^{\min}, T_2^{\max})\}$={(0.6,0.8),(0.8.0.9)}							
(40,20)	(30,15)	I	2.170	0.920	2.477	0.917	0.410	0.911	0.459	0.911
		II	2.145	0.921	2.474	0.918	0.327	0.927	0.377	0.929
		III	2.272	0.916	2.731	0.909	0.413	0.911	0.459	0.911
		IV	2.113	0.922	2.422	0.919	0.326	0.927	0.375	0.930
(40,30)	(30,25)	I	2.095	0.922	2.378	0.921	0.309	0.928	0.372	0.933
		II	2.056	0.924	2.308	0.923	0.298	0.934	0.343	0.936
		III	2.098	0.922	2.381	0.921	0.313	0.927	0.374	0.932
		IV	2.040	0.924	2.288	0.924	0.281	0.939	0.313	0.939

Table 8. Interval assessments of δ.

(n_1, m_1)	(n_2, m_2)	Test	ACI				BCI			
			LF		SF		LFBA		SFBA	
Group–A→			$\{(T_1^{\min}, T_1^{\max}), (T_2^{\min}, T_2^{\max})\}$={(0.3,0.8),(0.5.1.2)}							
(40,20)	(30,15)	I	0.402	0.925	0.412	0.924	0.263	0.930	0.296	0.930
		II	0.410	0.923	0.423	0.923	0.270	0.919	0.343	0.928
		III	0.426	0.920	0.453	0.917	0.287	0.915	0.360	0.923
		IV	0.407	0.924	0.414	0.924	0.266	0.921	0.337	0.929
(40,30)	(30,25)	I	0.359	0.933	0.368	0.933	0.243	0.933	0.284	0.935
		II	0.371	0.931	0.375	0.931	0.258	0.932	0.291	0.931
		III	0.397	0.926	0.404	0.926	0.263	0.930	0.296	0.930
		IV	0.360	0.933	0.369	0.932	0.245	0.932	0.289	0.935
Group–A→			$\{(T_1^{\min}, T_1^{\max}), (T_2^{\min}, T_2^{\max})\}$={(0.5,1.0),(0.8.1.5)}							
(40,20)	(30,15)	I	0.366	0.927	0.377	0.926	0.259	0.930	0.293	0.930
		II	0.402	0.920	0.408	0.920	0.265	0.917	0.348	0.929
		III	0.415	0.917	0.422	0.917	0.271	0.912	0.371	0.927
		IV	0.369	0.926	0.379	0.926	0.262	0.918	0.347	0.929
(40,30)	(30,25)	I	0.325	0.935	0.334	0.935	0.243	0.935	0.275	0.934
		II	0.336	0.933	0.340	0.933	0.257	0.931	0.289	0.931
		III	0.361	0.928	0.372	0.927	0.258	0.931	0.289	0.930
		IV	0.330	0.934	0.340	0.933	0.248	0.934	0.279	0.933
Group–B→			$\{(T_1^{\min}, T_1^{\max}), (T_2^{\min}, T_2^{\max})\}$={(0.4,0.6),(0.6.0.8)}							
(40,20)	(30,15)	I	0.790	0.923	0.819	0.923	0.435	0.930	0.514	0.934
		II	0.803	0.922	0.838	0.921	0.438	0.929	0.521	0.934
		III	0.855	0.917	0.877	0.917	0.439	0.929	0.526	0.933
		IV	0.794	0.923	0.832	0.921	0.436	0.929	0.524	0.934
(40,30)	(30,25)	I	0.692	0.933	0.718	0.932	0.410	0.935	0.479	0.938
		II	0.707	0.931	0.724	0.932	0.434	0.935	0.482	0.934
		III	0.755	0.927	0.790	0.925	0.435	0.934	0.485	0.934
		IV	0.695	0.932	0.718	0.932	0.421	0.935	0.480	0.936
Group–B→			$\{(T_1^{\min}, T_1^{\max}), (T_2^{\min}, T_2^{\max})\}$={(0.6,0.8),(0.8.0.9)}							
(40,20)	(30,15)	I	0.656	0.928	0.663	0.929	0.435	0.929	0.526	0.935
		II	0.803	0.912	0.835	0.910	0.447	0.928	0.533	0.933
		III	0.851	0.907	0.866	0.907	0.455	0.928	0.538	0.932
		IV	0.687	0.925	0.705	0.924	0.440	0.929	0.530	0.934
(40,30)	(30,25)	I	0.571	0.936	0.577	0.938	0.410	0.937	0.468	0.938
		II	0.607	0.930	0.614	0.934	0.425	0.933	0.498	0.936
		III	0.636	0.928	0.661	0.929	0.431	0.931	0.516	0.935
		IV	0.594	0.933	0.599	0.936	0.419	0.935	0.485	0.937

Table 9. Interval assessments of $\mathcal{R}$.

(n_1, m_1)	(n_2, m_2)	Test	ACI				BCI			
			LF		SF		LFBA		SFBA	
Group–A→			$\{(T_1^{\min}, T_1^{\max}), (T_2^{\min}, T_2^{\max})\}$={(0.3,0.8),(0.5.1.2)}							
(40,20)	(30,15)	I	0.345	0.938	0.327	0.935	0.133	0.949	0.129	0.950
		II	0.356	0.929	0.334	0.931	0.136	0.947	0.144	0.947
		III	0.350	0.933	0.332	0.935	0.134	0.949	0.134	0.947
		IV	0.370	0.928	0.342	0.928	0.138	0.945	0.148	0.946
(40,30)	(30,25)	I	0.311	0.959	0.296	0.964	0.115	0.953	0.109	0.953
		II	0.334	0.955	0.319	0.955	0.126	0.952	0.117	0.951
		III	0.333	0.956	0.318	0.957	0.120	0.952	0.111	0.951
		IV	0.340	0.952	0.325	0.952	0.130	0.951	0.123	0.950
Group–A→			$\{(T_1^{\min}, T_1^{\max}), (T_2^{\min}, T_2^{\max})\}$={(0.5,1.0),(0.8.1.5)}							
(40,20)	(30,15)	I	0.320	0.945	0.307	0.947	0.119	0.948	0.101	0.948
		II	0.330	0.930	0.318	0.935	0.130	0.947	0.107	0.946
		III	0.325	0.940	0.311	0.942	0.123	0.947	0.103	0.946
		IV	0.348	0.923	0.324	0.928	0.135	0.946	0.111	0.945
(40,30)	(30,25)	I	0.299	0.955	0.287	0.957	0.099	0.952	0.096	0.952
		II	0.311	0.952	0.296	0.956	0.110	0.950	0.098	0.949
		III	0.306	0.955	0.294	0.956	0.106	0.950	0.097	0.949
		IV	0.317	0.948	0.302	0.954	0.114	0.949	0.099	0.949
Group–B→			$\{(T_1^{\min}, T_1^{\max}), (T_2^{\min}, T_2^{\max})\}$={(0.4,0.6),(0.6.0.8)}							
(40,20)	(30,15)	I	0.292	0.918	0.284	0.922	0.073	0.945	0.066	0.943
		II	0.312	0.912	0.290	0.911	0.079	0.941	0.071	0.939
		III	0.299	0.915	0.287	0.919	0.076	0.942	0.068	0.942
		IV	0.326	0.908	0.310	0.910	0.085	0.939	0.076	0.938
(40,30)	(30,25)	I	0.258	0.927	0.247	0.931	0.061	0.951	0.052	0.952
		II	0.284	0.923	0.279	0.930	0.066	0.947	0.059	0.949
		III	0.268	0.925	0.257	0.931	0.064	0.950	0.054	0.951
		IV	0.287	0.920	0.280	0.927	0.069	0.946	0.061	0.945
Group–B→			$\{(T_1^{\min}, T_1^{\max}), (T_2^{\min}, T_2^{\max})\}$={(0.6,0.8),(0.8.0.9)}							
(40,20)	(30,15)	I	0.282	0.918	0.273	0.926	0.070	0.941	0.059	0.940
		II	0.297	0.912	0.289	0.917	0.075	0.940	0.066	0.938
		III	0.288	0.916	0.281	0.918	0.073	0.940	0.062	0.939
		IV	0.308	0.911	0.292	0.912	0.077	0.939	0.071	0.938
(40,30)	(30,25)	I	0.236	0.925	0.227	0.928	0.055	0.945	0.050	0.943
		II	0.257	0.921	0.247	0.927	0.057	0.942	0.056	0.940
		III	0.244	0.924	0.235	0.928	0.056	0.944	0.054	0.942
		IV	0.268	0.919	0.257	0.926	0.061	0.941	0.057	0.940

6. Organic white LED

A light-emitting diode (LED) is a solid-state electronic component that generates light through electroluminescence when an electric current passes through it. Unlike traditional incandescent bulbs, LEDs are energy-efficient, compact, and long-lasting, making them ideal for a wide range of applications. Depending on the materials used, LEDs can emit light in the visible, ultraviolet, or infrared spectrum. Organic white LEDs (WOLEDs) are a promising low-power lighting technology due to their high efficiency and low manufacturing costs. The large surfaces of WOLEDs emit high-quality white light, making them attractive for low-power lighting applications. This application demonstrates the applicability of proposed methodologies for evaluating the lifetime of M00071 WOLEDs mixed with red, green, and blue colors under two stress levels, called: 9.64mA (with $n_1 = 10$) and 17.09mA (with $n_2 = 10$). This WOLED dataset was originally reported by Zhang et al. [31] and analyzed later by Nassar et al. [32], Nassar et al. [33], and Alotaibi et al. [34]. For computing reasons, Table 10 divides each WOLED data point by two thousands.

Table 10. Times to failure of 10 M00071 WOLED datasets.

Group	Data									
X (9.64mA)	0.84575	1.04235	1.05015	1.18725	1.21075	1.29300	1.31075	1.34025	1.43400	1.43975
Y (17.09mA)	0.30075	0.34485	0.34865	0.35825	0.39275	0.42725	0.44475	0.55785	0.56565	0.62575

Given the growing importance of WOLEDs in everyday life and to show the value of our statistical approach, we analyze lifetime data collected under two specific stress levels. To see if the Weibull distribution is a good fit for this data, to calculate the Kolmogorov-Smirnov (K-S) test statistic and its $\mathcal{P}$-value, we first calculate the MLEs for the Weibull parameters $\theta_i,\ i = 1, 2$, and δ, along with their standard errors (Std.Es). Besides them, we also compute 95% ACIs (LF-based) along with their interval lengths (ILs); see Table 11. Since the P-value is much larger than the usual significance level of $\alpha = 0.05$, we conclude that the Weibull model fits the M00071 WOLED datasets well. A detailed check of how well the model fits the WOLED datasets is shown in Figure 1, using four popular visual tools: (1) empirical and estimated reliability lines; (2) empirical and estimated probability-probability (PP) lines; (3) empirical and estimated quantile-quantile (QQ) lines; and (4) contour map of the log-likelihood function. For both groups, X and Y, the plots in Figure 1(a)–(c) show a strong match between the real data and the fitted Weibull model, suggesting a superior fit. The total time on test (TTT) plots in the contour diagram in Figure 1(d) confirm that the fitted values of $\hat{\theta}_i,\ i = 1, 2$, and $\hat{\delta}$ exist, are unique, and can be reliably used as starting points for forthcoming analysis.

One of the main objectives of the study is to evaluate the reliability behavior of the Weibull stress strength using different samples collected according to the proposed IAPT2C mechanism terminology discussed in Section 1. To achieve that, from the M00071 WOLED data groups listed in Table 10, several artificial IAPT2C samples (denoted by $\mathbb{S}[i],\ i = 1, 2, 3$) are generated using $m_1 = m_2 = 5$, $(\mathbf{R}, \mathbf{Q}) = \{(1^*5), (1^*5)\}$, and different combinations of threshold limits ($T_i^{\min}$ and $T_i^{\max}$ for $i = 1, 2$); see Table 12. For $\mathbb{S}[i],\ i = 1, 2, 3$, we evaluate the proposed point estimates (with standard errors) and 95% interval estimates (with interval lengths) for the model parameters $\theta_i,\ i = 1, 2$, and δ and the

stress-strength reliability measure $\mathcal{R}$ using ML, MPS, LFBA, and SFBA methods; see Table 13.

Since we lack prior knowledge about the Weibull parameters for the M00071 WOLED datasets, all point and credible Bayesian analyses (LFBA and SFBA) use a joint improper gamma prior. For the MCMC procedure, we set the number of iterations to 50,000 and use a burn-in of 10,000 iterations. The MLEs (MPSE) of $\theta_i,\ i = 1, 2$, and δ (listed in Table 13) serve as the initial values for the LFBA (SFBA) method.

Table 11. Fitting results of Weibull lifespan model from M00071 WOLED datasets.

Group	Par.	MLE(Std.E)	95% ACI			K–S($\mathcal{P}$-Value)
			Low.	Upp.	IL	
X	δ	8.5408(2.2241)	4.1833	12.895	8.7124	0.1416(0.9716)
	θ_1	0.1135(0.0839)	0.0000	0.2778	0.2778	
Y	δ	4.4599(1.0770)	2.3504	6.5605	4.2101	0.1865(0.8168)
	θ_2	26.767(20.078)	0.0000	65.732	65.732	

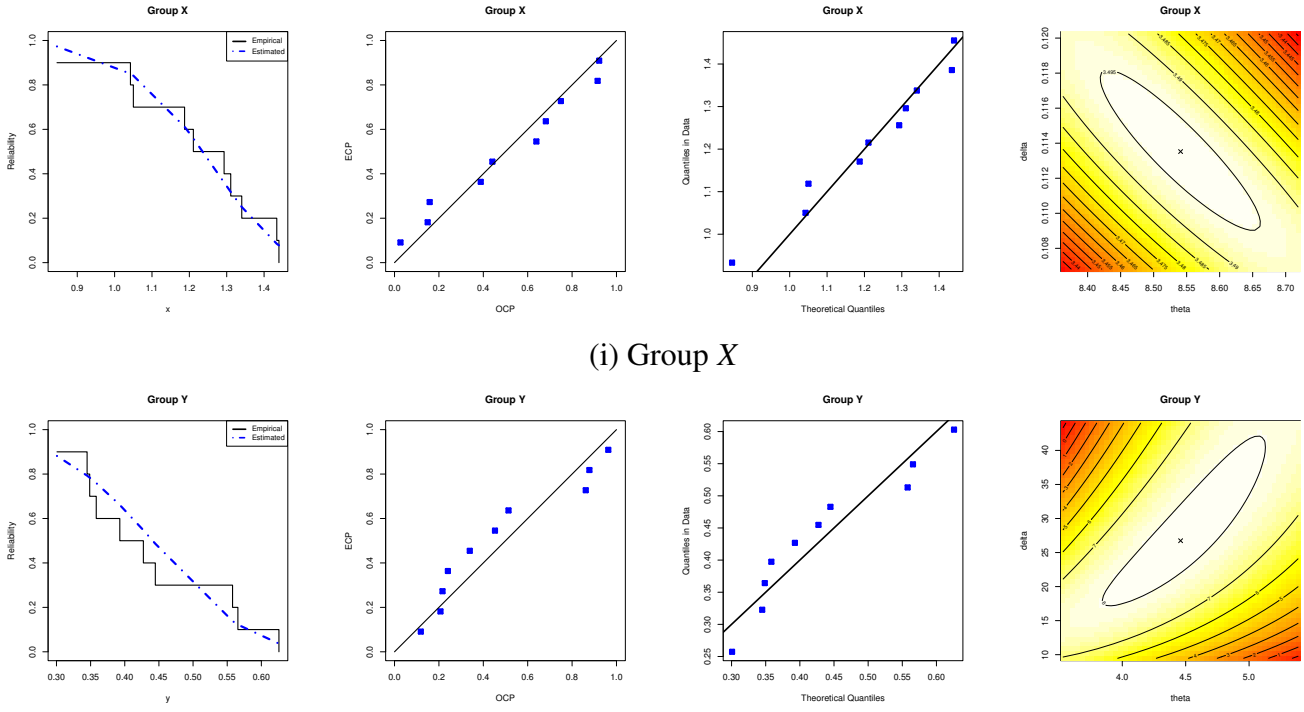

(i) Group X

(ii) Group Y

(a) PDF (b) RF (c) PP (d) Contour

Figure 1. Four data representations of the Weibull lifespan model from M00071 WOLED datasets.

It is clear, from Table 13, that the MCMC-based estimates from the LFBA (or SFBA) method for

θ_i, $i = 1, 2$, δ, and $\mathcal{R}$ show favorable behavior and outperform the competitive frequentist estimates from the ML (or MPS) method, particularly with respect to their smaller standard errors. Similar facts are observed when comparing the BCIs through LFBA/SFBA to the ACIs through LF/SF, with the former generally producing shorter interval widths, indicating greater precision.

In addition, Table 14 provides a detailed summary of key descriptive statistics for the Weibull parameters, including the mean, mode, quartiles (symbolized by $\mathbb{Q}i$ for $i = 1, 2, 3$), standard deviation (Std.D), and skewness (Skew.). These summary measures support the same conclusions previously shown in Table 13.

Table 12. Artificial IAPT2C samples from M00071 WOLED datasets.

Sample	$T_1^{\min}(d_1)$ $T_2^{\min}(d_2)$	$T_1^{\max}(r_1)$ $T_2^{\max}(r_2)$	$\underline{\mathbf{x}}$ $\underline{\mathbf{y}}$	$(R^\star,Q^\star)$	(τ_1, τ_2)
$\mathbb{S}[1]$	1.45(5)	1.55(5)	0.84575, 1.04235, 1.21075, 1.29300, 1.43400	(0,0)	(1.43400, 0.55785)
	0.60(5)	0.65(5)	0.30075, 0.34485, 0.35825, 0.39275, 0.55785		
$\mathbb{S}[2]$	1.30(3)	1.32(4)	0.84575, 1.21075, 1.29300, 1.31075	(3,3)	(1.32, 0.45)
	0.40(3)	0.45(4)	0.30075, 0.34485, 0.39275, 0.44475		
$\mathbb{S}[3]$	0.85(2)	1.35(4)	0.84575, 1.05015, 1.29300, 1.34025	(4,4)	(1.35, 0.60)
	0.35(2)	0.60(4)	0.30075, 0.34865, 0.42725, 0.56565		

Table 13. Estimates of $\theta_i,\ i = 1, 2$, δ, and $\mathcal{R}$ from M00071 WOLED datasets.

Sample	Par.	MLE / MPSE		MCMC (LFBA) / MCMC (SFBA)		95% ACI-LF / 95% ACI-SF			95% BCI-LF / 95% BCI-SF		
		Est.	SE	Est.	SE	Low.	Upp.	IL	Low.	Upp.	IL
$\mathbb{S}[1]$	θ_1	4.7401	1.3207	4.7390	0.0101	2.1515	7.3287	5.1772	4.7195	4.7587	0.0392
		5.7625	1.7911	5.7616	0.0100	2.2520	9.2730	7.0210	5.7420	5.7813	0.0393
	θ_2	1.2557	0.5089	1.2546	0.0100	0.2583	2.2532	1.9948	1.2353	1.2743	0.0390
		1.2163	0.5558	1.2151	0.0101	0.1269	2.3057	2.1788	1.1954	1.2349	0.0395
	δ	0.5933	0.2345	0.5921	0.0101	0.1336	1.0529	0.9193	0.5725	0.6119	0.0394
		0.5255	0.2406	0.5243	0.0101	0.0540	0.9971	0.9431	0.5048	0.5441	0.0392
	$\mathcal{R}$	0.7906	0.0850	0.7907	0.0014	0.6240	0.9571	0.3331	0.7880	0.7933	0.0053
		0.8257	0.0829	0.8258	0.0012	0.6633	0.9882	0.3249	0.8235	0.8282	0.0047
$\mathbb{S}[2]$	θ_1	4.0243	1.5672	4.0232	0.0101	0.9525	7.0960	6.1435	4.0036	4.0428	0.0392
		4.4839	2.0532	4.4830	0.0100	0.4598	8.5080	8.0482	4.4634	4.5027	0.0393
	θ_2	1.2321	0.5583	1.2309	0.0101	0.1379	2.3262	2.1883	1.2116	1.2506	0.0390
		1.2052	0.6404	1.2040	0.0101	0.0050	2.4604	2.4554	1.1843	1.2238	0.0395
	δ	0.3729	0.1763	0.3717	0.0101	0.0273	0.7185	0.6912	0.3521	0.3914	0.0393
		0.2827	0.1671	0.2814	0.0100	0.0045	0.6102	0.6057	0.2619	0.3010	0.0392
	$\mathcal{R}$	0.7656	0.1138	0.7657	0.0015	0.5427	0.9886	0.4459	0.7627	0.7687	0.0059
		0.7882	0.1246	0.7883	0.0014	0.5439	1.0324	0.4885	0.7855	0.7911	0.0056
$\mathbb{S}[3]$	θ_1	3.3774	1.3667	3.3763	0.0101	0.6988	6.0560	5.3573	3.3567	3.3960	0.0392
		3.5417	1.6519	3.5408	0.0100	0.3040	6.7793	6.4753	3.5212	3.5604	0.0393
	θ_2	1.3600	0.6230	1.3589	0.0101	0.1389	2.5812	2.4422	1.3396	1.3786	0.0390
		1.3325	0.7143	1.3313	0.0101	0.0167	2.7324	2.7156	1.3116	1.3511	0.0395
	δ	0.3607	0.1647	0.3594	0.0101	0.0379	0.6834	0.6455	0.3398	0.3792	0.0393
		0.2868	0.1553	0.2855	0.0100	0.0176	0.5913	0.5736	0.2661	0.3052	0.0391
	$\mathcal{R}$	0.7129	0.1326	0.7130	0.0016	0.4530	0.9728	0.5198	0.7098	0.7161	0.0063
		0.7266	0.1499	0.7267	0.0016	0.4328	1.0205	0.5877	0.7236	0.7299	0.0063

Table 14. Statistics of $\theta_i,\ i = 1, 2$, δ, and $\mathcal{R}$ from M00071 WOLED data.

Sample	Par.	Mean	Mode	$\mathbb{Q}1$	$\mathbb{Q}2$	$\mathbb{Q}3$	Std.D	Skew.
				MCMC (LFBA)				
				MCMC (SFBA)				
$\mathbb{S}[1]$	θ_1	4.7390	4.7149	4.7323	4.7390	4.7458	0.0100	0.0148
		5.7616	5.7547	5.7549	5.7616	5.7682	0.0100	0.0225
	θ_2	1.2546	1.2289	1.2478	1.2545	1.2613	0.0100	0.0228
		1.2151	1.1963	1.2084	1.2151	1.2219	0.0100	0.0099
	δ	0.5921	0.5808	0.5854	0.5921	0.5989	0.0101	-0.0113
		0.5243	0.5166	0.5176	0.5243	0.5310	0.0100	0.0209
	$\mathcal{R}$	0.7907	0.7895	0.7898	0.7907	0.7916	0.0014	-0.0296
		0.8258	0.8279	0.8250	0.8258	0.8266	0.0012	-0.0061
$\mathbb{S}[2]$	θ_1	4.0232	4.0102	4.0164	4.0231	4.0300	0.0100	0.0156
		4.4830	4.4761	4.4763	4.4830	4.4896	0.0100	0.0244
	θ_2	1.2309	1.1977	1.2241	1.2309	1.2377	0.0100	0.0187
		1.2040	1.1852	1.1974	1.2040	1.2108	0.0100	0.0089
	δ	0.3717	0.3627	0.3649	0.3716	0.3784	0.0100	-0.0118
		0.2814	0.2737	0.2746	0.2813	0.2880	0.0100	0.0160
	$\mathcal{R}$	0.7657	0.7700	0.7647	0.7657	0.7668	0.0015	-0.0291
		0.7883	0.7906	0.7873	0.7883	0.7893	0.0014	-0.0027
$\mathbb{S}[3]$	θ_1	3.3763	3.3633	3.3695	3.3763	3.3831	0.0100	0.0155
		3.5408	3.5339	3.5341	3.5407	3.5474	0.0100	0.0241
	θ_2	1.3589	1.3257	1.3521	1.3589	1.3657	0.0100	0.0182
		1.3313	1.3125	1.3246	1.3313	1.3381	0.0100	0.0090
	δ	0.3594	0.3505	0.3527	0.3594	0.3662	0.0100	-0.0125
		0.2855	0.2779	0.2788	0.2855	0.2922	0.0100	0.0174
	$\mathcal{R}$	0.7130	0.7173	0.7119	0.7130	0.7141	0.0016	-0.0330
		0.7267	0.7292	0.7257	0.7267	0.7278	0.0016	-0.0019

To verify the existence and uniqueness of the estimates obtained from ML and MPS methodologies for $\theta_i,\ i = 1, 2$, δ, and $\mathcal{R}$ reported in Table 13, contour diagrams of $\theta_i,\ i = 1, 2$, and δ are created from $\mathbb{S}[i],\ i = 1, 2, 3$; see Figures 2–3. These diagrams confirm that the MLEs (MPSEs) of $\theta_i,\ i = 1, 2$, and δ exist and are unique. Using $\mathbb{S}[1]$ as an illustrative example, Figure 4 presents the trace and posterior density plots for $\theta_i,\ i = 1, 2$, δ, and $\mathcal{R}$ based on their 40,000 MCMC draws post-burn-in. The trace and density plots (shown in Figure 4) show good mixing of the MCMC chains, and the posterior densities appear roughly symmetric, supporting the stability and reliability of the Bayesian inference.

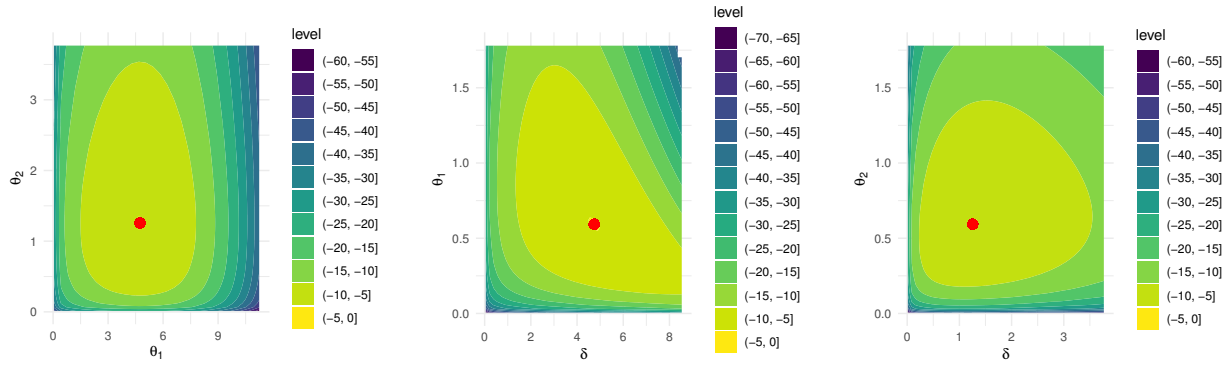

(a) Sample $\mathbb{S}[1]$

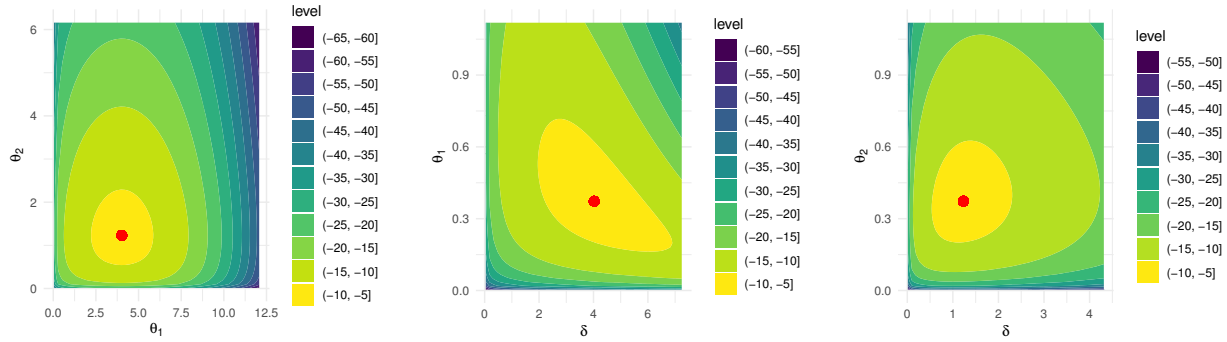

(b) Sample $\mathbb{S}[2]$

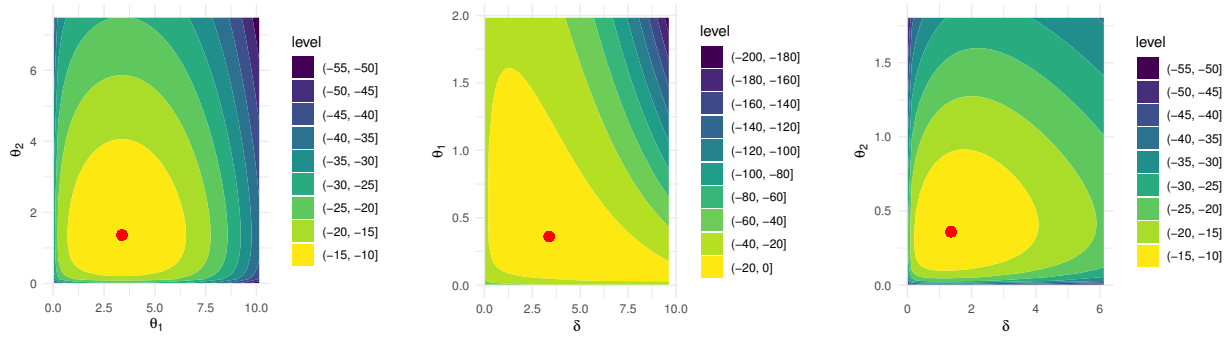

(c) Sample $\mathbb{S}[3]$

Figure 2. Contours from log-LF for $\theta_i,\ i = 1, 2$, and δ from M00071 WOLED datasets.

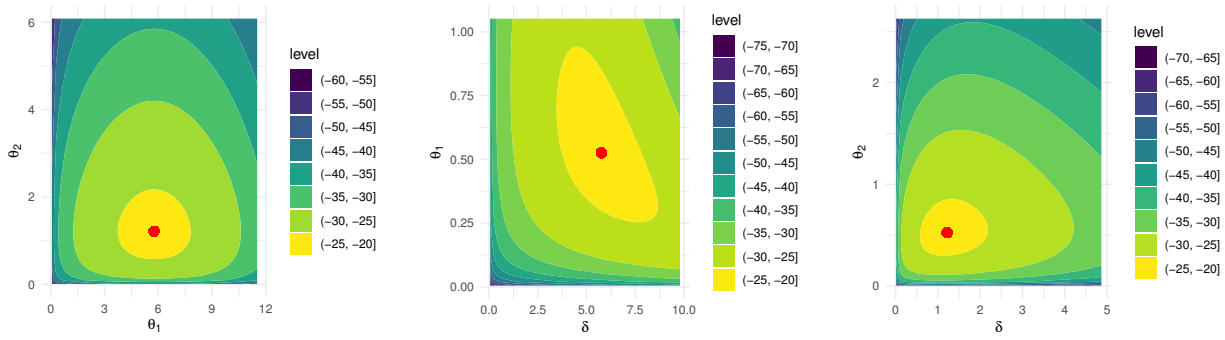

(a) Sample $\mathbb{S}[1]$

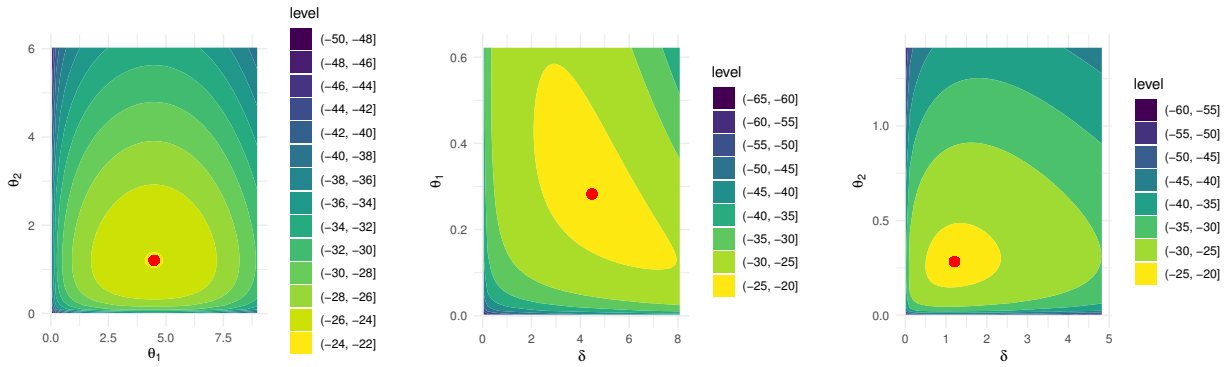

(b) Sample $\mathbb{S}[2]$

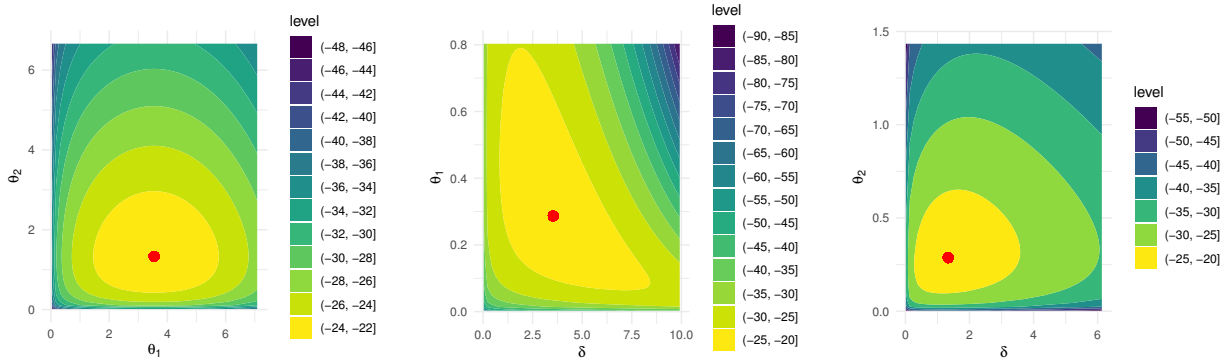

(c) Sample $\mathbb{S}[3]$

Figure 3. Contours from log-SF for $\theta_i,\ i = 1, 2$, and δ from M00071 WOLED datasets.

In conclusion, the analysis of M00071 WOLEDs under two stress levels confirms their suitability for reliability studies using statistical lifetime modeling. It is recommended that future research continue to apply and refine these methodologies across varied operating conditions to further enhance predictive accuracy and support the development of robust, energy-efficient lighting technologies.

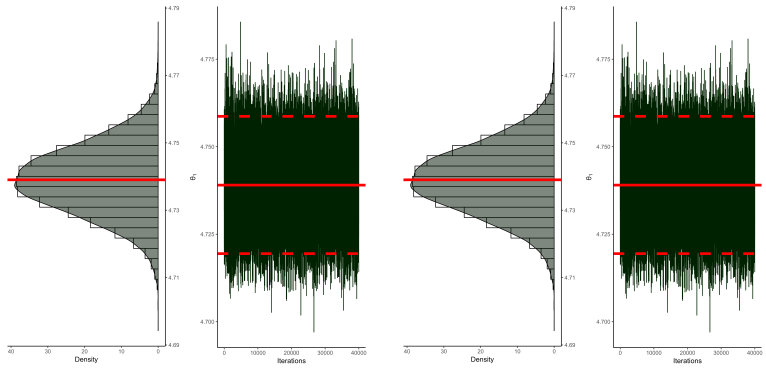

(a) θ_1

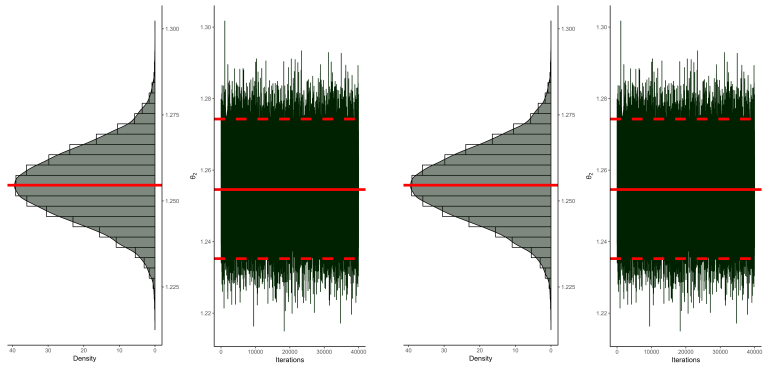

(b) θ_2

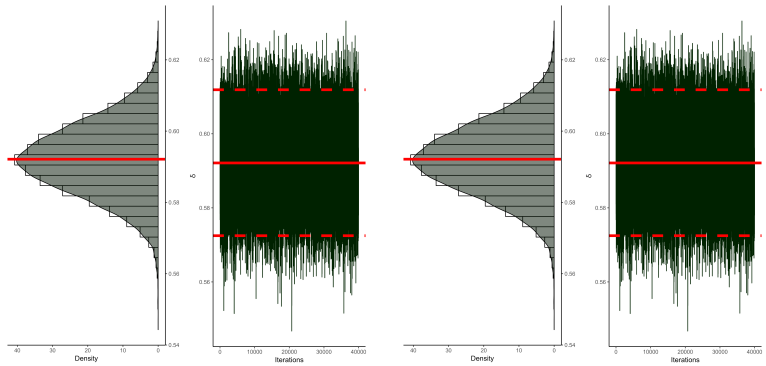

(c) δ

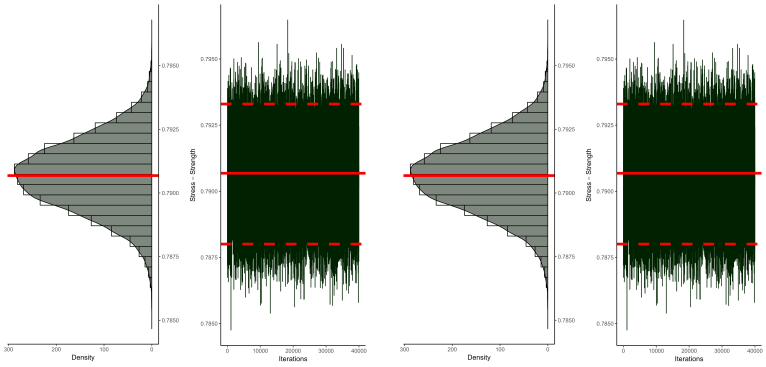

(d) $\mathcal{R}$

(i) MCMC (LFBA) (ii) MCMC (SFBA)

Figure 4. The MCMC diagrams of $\theta_i,\ i = 1, 2, \delta$, and $\mathcal{R}$ from M00071 WOLED datasets.

7. Concluding remarks

This study explored a range of classical and Bayesian estimation techniques for inferring the stress-strength reliability parameter under an improved adaptive progressive Type-II censoring scheme. The underlying reliability model assumed that the stress and strength variables are independently Weibull-distributed, sharing a common shape parameter but differing in their scale parameters. A central contribution of this work is the integration of the maximum product of spacings method within the considered censoring framework, alongside the conventional MLE and two Bayesian approaches based on the likelihood and spacings functions. For Bayesian inference, posterior estimates were obtained under the squared error loss function, assuming independent gamma priors for all model parameters. Posterior sampling for the likelihood-based Bayesian approach was implemented using an M–H algorithm embedded within a Gibbs sampling framework, whereas the spacing-based Bayesian method relied solely on the M–H algorithm. Simulation studies highlighted the numerical accuracy and efficiency of the proposed estimators, with the Bayesian methods demonstrating strong performance due to their capacity to incorporate prior information. The practical utility of the approaches was further illustrated through a real-data application representing the times to failure of organic white light-emitting diodes, confirming the relevance and effectiveness of the proposed methodologies in applied reliability analysis.

Author contributions

Refah Alotaibi: Conceptualization, methodology, investigation, funding acquisition, writing – original draft; Ahmed Elshahhat: Methodology, writing – original draft, writing – review & editing; Mazen Nassar: Conceptualization, methodology, writing – review & editing. All authors read and approved the final manuscript.

Use of Generative-AI tools declaration

The authors declare they have not used Artificial Intelligence (AI) tools in the creation of this article.

Acknowledgments

This research was funded by Princess Nourah bint Abdulrahman University Researchers Supporting Project number (PNURSP2025R50), Princess Nourah bint Abdulrahman University, Riyadh, Saudi Arabia.

Conflicts of interest

The authors declare no conflict of interest.

References

1. Z. W. Birnbaum, On a use of the Mann–Whitney statistic, *Proc. 3rd Berkeley Symp. Math. Stat. Probab.*, Univ. California Press, Berkeley, **1** (1956), 13–17.

2. S. Kotz, Y. Lumelskii, M. Pensky, *The stress–strength model and its generalizations: Theory and applications*, World Scientific, New York, 2003.

3. V. K. Sharma, S. K. Singh, U. Singh, V. Agiwal, The inverse Lindley distribution: A stress-strength reliability model with application to head and neck cancer data, *J. Ind. Prod. Eng.,* **32** (2015), 162–173. https://doi.org/10.1080/21681015.2015.1025901

4. V. K. Sharma, Bayesian analysis of head and neck cancer data using generalized inverse Lindley stress-strength reliability model, *Commun. Stat. Theor.- M.,* **47** (2018), 1155–1180. https://doi.org/10.1080/03610926.2017.1316858

5. F. S. Quintino, M. Oliveira, P. N. Rathie, L. C. Ozelim, T. A. da Fonseca, Asset selection based on estimating stress-strength probabilities: The case of returns following three-parameter generalized extreme value distributions, *AIMS Math.,* **9** (2024), 2345–2368. https://doi.org/10.3934/math.2024116

6. M. S. Kotb, M. A. Al Omari, Estimation of the stress-strength reliability for the exponential-Rayleigh distribution, *Math. Comput. Simulat.,* **228** (2025), 263–273. https://doi.org/10.1016/j.matcom.2024.09.005

7. L. Wang, Y. Yu, Y. Lio, Y. M. Tripathi, Analysis of stress-strength reliability from a generalized exponential distribution under maximum ranked set sampling with unequal samples, *J. Stat. Comput. Simul.,* **95** (2025), 1944–1975. https://doi.org/10.1080/00949655.2025.2476019

8. H. Rinne, *The Weibull distribution: A handbook*, Chapman Hall/CRC, 2008.

9. E. Chiodo, G. Mazzanti, Bayesian reliability estimation based on a Weibull stress-strength model for aged power system components subjected to voltage surges, *IEEE Trans. Dielectr. Electr. Insul.,* **13** (2006), 146–159. https://doi.org/10.1109/TDEI.2006.1593413

10. A. Asgharzadeh, R. Valiollahi, M. Z. Raqab, Stress-strength reliability of Weibull distribution based on progressively censored samples, *SORT-Stat. Oper. Res. T.,* **35** (2011), 103–124. https://hdl.handle.net/2099/13276

11. B. X. Wang, Z. S. Ye, Inference on the Weibull distribution based on record values, *Comput. Stat. Data Anal.,* **83** (2015), 26–36. https://doi.org/10.1016/j.csda.2014.09.005

12. A. M. Almarashi, A. Algarni, M. Nassar, On estimation procedures of stress-strength reliability for Weibull distribution with application, *PLoS One,* **15** (2020), e0237997. https://doi.org/10.1371/journal.pone.0237997

13. N. Balakrishnan, R. Aggarwala, *Progressive censoring: Theory, methods, and applications*, Springer Science & Business Media, 2000.

14. N. Balakrishnan, Progressive censoring methodology: An appraisal, *Test,* **16** (2007), 211–259. https://doi.org/10.1007/s11749-007-0061-y

15. D. Kundu, A. Joarder, Analysis of Type-II progressively hybrid censored data, *Comput. Stat. Data Anal.,* **50** (2006), 2509–2528. https://doi.org/10.1016/j.csda.2005.05.002

16. H. K. T. Ng, D. Kundu, P. S. Chan, Statistical analysis of exponential lifetimes under an adaptive Type-II progressive censoring scheme, *Naval Res. Logist.,* **56** (2009), 687–698. https://doi.org/10.1002/nav.20371

17. M. Nassar, O. E. Abo-Kasem, Estimation of the inverse Weibull parameters under adaptive type-II progressive hybrid censoring scheme, *J. Comput. Appl. Math.,* **315** (2017), 228–239. https://doi.org/10.1016/j.cam.2016.11.012

18. S. Dutta, S. Dey, S. Kayal, Bayesian survival analysis of logistic exponential distribution for adaptive progressive Type-II censored data, *Comput. Stat.,* **39** (2024), 2109–2155. https://doi.org/10.1007/s00180-023-01376-y

19. C. Zhang, J. Zhang, W. Gui, Bayesian inference for Marshall-Olkin bivariate Lomax-Geometric distribution under adaptive type-II progressive hybrid censored dependent competing risks data, *Commun. Stat. Simul. Comput.,* 2025, 1–22. https://doi.org/10.1080/03610918.2025.2474597

20. W. Yan, P. Li, Y. Yu, Statistical inference for the reliability of Burr-XII distribution under improved adaptive Type-II progressive censoring, *Appl. Math. Model.,* **95** (2021), 38–52. https://doi.org/10.1016/j.apm.2021.01.050

21. M. Nassar, A. Elshahhat, Estimation procedures and optimal censoring schemes for an improved adaptive progressively type-II censored Weibull distribution, *J. Appl. Stat.,* **51** (2024), 1664–1688. https://doi.org/10.1080/02664763.2023.2230536

22. L. Zhang, R. Yan, Parameter estimation of Chen distribution under improved adaptive Type-II progressive censoring, *J. Stat. Comput. Simul.,* **94** (2024), 2830–2861. https://doi.org/10.1080/00949655.2024.2358828

23. C. Swaroop, S. Dutta, S. Saini, N. Tiwari, Estimation of stress-strength reliability for the generalized inverted exponential distribution based on improved adaptive Type-II progressive censoring, *Comput. Stat.,* 2025, 1–37. https://doi.org/10.1007/s00180-025-01612-7

24. M. Irfan, S. Dutta, A. K. Sharma, Statistical inference and optimal plans for improved adaptive Type-II progressive censored data following Kumaraswamy-G family of distributions, *Phys. Scr.,* **100** (2025), 025213. https://doi.org/10.1088/1402-4896/ada216

25. R. C. H. Cheng, N. A. K. Amin, Estimating parameters in continuous univariate distributions with a shifted origin, *J. Roy. Stat. Soc. Ser. B (Methodol.),* **45** (1983), 394–403. https://doi.org/10.1111/j.2517-6161.1983.tb01268.x

26. B. Ranneby, The maximum spacing method: An estimation method related to the maximum likelihood method, *Scand. J. Stat.,* **11** (1984), 93–112. Available from: `https://www.jstor.org/stable/4615946`.

27. S. Anatolyev, G. Kosenok, An alternative to maximum likelihood based on spacings, *Economet. Theor.,* **21** (2005), 472–476. https://doi.org/10.1017/S0266466605050255

28. T. Kurdi, M. Nassar, F. M. A. Alam, Bayesian estimation using product of spacing for modified Kies exponential progressively censored data, *Axioms,* **12** (2023), 917. https://doi.org/10.3390/axioms12100917

29. A. Henningsen, O. Toomet, MaxLik: A package for maximum likelihood estimation in R, *Comput. Stat.,* **26** (2011), 443–458. https://doi.org/10.1007/s00180-010-0217-1

30. M. Plummer, N. Best, K. Cowles, K. Vines, CODA: convergence diagnosis and output analysis for MCMC, *R News,* **6** (2006), 7–11.

31. J. Zhang, G. Cheng, X. Chen, Y. Han, T. Zhou, Y. Qiu, Accelerated life test of white OLED based on lognormal distribution, *Indian J. Pure Appl. Phys.,* **52** (2015), 671–677.

32. M. Nassar, S. Dey, L. Wang, A. Elshahhat, Estimation of Lindley constant-stress model via product of spacing with Type-II censored accelerated life data, *Commun. Stat. Simul. Comput.,* **53** (2024), 288–314. https://doi.org/10.1080/03610918.2021.2018460

33. M. Nassar, R. Alotaibi, A. Elshahhat, Reliability analysis at usual operating settings for Weibull constant-stress model with improved adaptive type-II progressively censored samples, *AIMS Math.,* **9** (2024), 16931–16965. https://doi.org/10.3934/math.2024823

34. R. Alotaibi, M. Nassar, Z. A. Khan, A. Elshahhat, Statistical analysis of stress–strength in a newly inverted Chen model from adaptive progressive type-II censoring and modelling on light-emitting diodes and pump motors, *AIMS Math.,* **9** (2024), 34311–34355. https://doi.org/10.3934/math.20241635

Supplementary

Table S1: Point assessments of θ_1 from Group–A; Table S2: Point assessments of θ_1 from Group–B; Table S3: Point assessments of θ_2 from Group–A; Table S4: Point assessments of θ_2 from Group–B; Table S5: Point assessments of δ from Group–A; Table S6: Point assessments of δ from Group–B; Table S7: Point assessments of $\mathcal{R}$ from Group–A; Table S8: Point assessments of $\mathcal{R}$ from Group–B; Table S9: Interval assessments of θ_1 from Group–A; Table S10: Interval assessments of θ_1 from Group–B; Table S11: Interval assessments of θ_2 from Group–A; Table S12: Interval assessments of θ_2 from Group–B; Table S13: Interval assessments of δ from Group–A; Table S14: Interval assessments of δ from Group–B; Table S15: Interval assessments of $\mathcal{R}$ from Group–A; Table S16: Interval assessments of $\mathcal{R}$ from Group–B.